Community composition, population structure and phylogeny of coastal sympagic meiofauna in eastern Svalbard

a master thesis by

Magnus Heide Andreasen

at the

Department of Arctic Biology

submitted

1st of June, 2019

Supervised by

Lise Øvreås

Professor
Dept. of Biological Sciences
The University in Bergen

and

Janne E. Søreide

Associate Professor
Dept. of Arctic Biology
The University Centre in Svalbard

UNIS
The University Centre in Svalbard

Table of contents

Acknowledgements i
List of figures ii
List of tables iii
List of equations iii
List of abbreviations iii

Abstract 1
Introduction 2
Materials and methods 5
  Field collection 5
  The physical environment 6
  Chlorophyll *a* 7
  Sympagic meiofauna 7
  Hydrography 8
  Pelagic meiofauna 8
  Length measurements 9
  DNA extraction, PCR and purification 9
  Bioinformatic analyses and phylogeny 10
Results 11
  The physical environment 11
  Hydrography and chlorophyll *a* 12
  Sympagic meiofauna 14
  Chlorophyll *a* and sympagic meiofauna 15
  Pelagic meiofauna 15
  Length measurements 16
  Phylogeny 16
Discussion 20
  Community composition 20
  Diversity of sympagic polychaetes and nematodes 22
  Further prospects 23
Conclusion 24
References 24
Supporting information 34

Acknowledgements

This thesis was written on Svalbard in the dark, in Copenhagen on a student café and on Bornholm in our family café by the sea. I am overly grateful for the inputs, discussions and laughs brought about by the company surrounding me whether it being in Norway or Denmark.

More specifically, I would like to thank Janne Elin Søreide for making this project possible, for solid guiding on the sea ice, for patience when sledges fell off and for thorough supervision during the writing process. Thank you Lise Øvreås for profound supervision from Bergen and for trusting us in sampling sea ice bacteria; I truly hope they turn out useful! Miriam Marquardt and Stuart Thomson; you have played a vital part in getting us started, and in keeping us afloat, in the molecular laboratories; thank you! I am grateful for the field assistance by Malin Daase. You make field trips memorable in the best possible way; sinking sea ice saws and polar bears top the list; thanks to you too. Thank you, Rupert Krapp, for guidance on the sea ice and for making sure the polar bear stayed away.

The Norwegian Polar Institute lent us their cabin in Inglefieldbukta during the two sea ice campaigns. Staying there was a privilege, thank you! The Norwegian Research Council funded the entire project. For that I cannot be grateful enough; thank you from here to the North Pole!

Margot Nyeggen, Vanessa Pitusi and Kirsa Nørregaard; I cannot thank you enough for the exceptional, numerous days in the field, in the lab and at Sjøskrenten – let there be many more to come. Thank you, Cassandra Debets, for stimulating discussions about science and life.

Rolf Gradinger, Eva Leu, Jósef M. Wiktor, Maja K. Hatlebakk and the students of the AB-330 course Ecosystems in Ice Covered Waters in spring 2018 all helped collecting physical data and biological samples in Agardhbukta. Thank you for that and for a stimulating, challenging and well-planned course. Thanks to the crew and students of the R/V Helmer Hansen cruise in early May 2018 for collecting nematode-containing sea ice. The cooperation between the University Centre in Svalbard and Hurtigruten allowed for sampling in Palanderbukta 18th of June 2018. Thanks to the crew and guides onboard M/S Spitsbergen for helping out obtaining these samples.

To my family and Olivia; thank you for providing the best imaginable surroundings during the writing process, for laughs and for endless support.

List of figures

Figure 1 Sampling stations in Inglefieldbukta (A; IB) and Agardhbukta (B; AGA) in eastern Svalbard, Norway.

Figure 2 Vertical sea ice profiles of salinity, temperature, brine salinity and brine volume in Inglefieldbukta (shallow station: IB1 and deep stations: IB2, IB3) in March and April and Agardhbukta (AGA) in April 2018. The dashed line marks the 5% theoretical minima in brine volume for meiofauna to occur (Golden et al. 1998).

Figure 3 CTD and fluorescence profiles in Inglefieldbukta in March (left) and April (right) at deep stations IB2 and IB3, respectively.

Figure 4 Integrated total and relative abundance of sympagic meiofauna in Inglefieldbukta (IB) and Agardhbukta (AGA) in eastern Svalbard, spring 2018. Poly. juv. = polychaete juvenile, Troch. larv. = trochophore larvae, Unident. = unidentified.

Figure 5 Sympagic meiofauna abundance (mean+SD; $n = 3$) and sympagic chlorophyll *a* (mean+SD; $n = 3$) in the lower 10 cm sections in Inglefieldbukta (IB1-3) and Agardhbukta (AGA) in eastern Svalbard, 2018. Poly. juv. = polychaete juvenile, Troch. larv. = trochophore larvae, Unident. = unidentified, Chl *a* = chlorophyll *a*. Note differences in scales.

Figure 6 Phylogenetic tree based on maximum likelihood (bold bootstrap values) and maximum parsimony (grey bootstrap values) on 10 polychaetes from Inglefieldbukta in April and 25 polychaetes from the Canadian Arctic. Accession numbers are available in Appendix 8 and reference names in Appendix 12. *Sequences from this study.

Figure 7 Phylogenetic tree based on maximum likelihood (bold bootstrap values) and neighbour joining (grey bootstrap values) on three polychaetes from Van Mijenfjorden April 2017 and 18 reference sequences mostly from the Canadian Arctic, Chukchi Sea and Svalbard. Accession numbers are available in Appendix 8 and reference names in Appendix 12. *Analysed in this study with sequences from Pitusi et al. (2019).

Figure 8 Phylogenetic tree based on maximum likelihood (bold bootstrap values) and maximum parsimony (grey bootstrap values) on seven nematodes from Inglefieldbukta (IB1-2), two from Palanderbukta (PAL), 44 from Van Mijenfjorden (VMF), 20 from the Netherlands (GD1-5; *Theristus*) and five from the Håkon Mosby Mud Volcano (HMMV). Accession numbers are available in Appendix 8 and reference names in Appendix 12. * Sequences from this study, ** Sequences from Pitusi (2019).

List of tables

Table 1 Average (± SD) measures of physical parameters (cm) of the sea ice and snow in Inglefieldbukta (IB) and Agardhbukta (AGA) in Svalbard.

List of equations

Equation 1 Brine salinity (Cox and Weeks 1983)

Equation 2 Brine volume (Cox and Weeks 1983)

Equation 3 Meiofauna individuals m^{-2} $section^{-1}$ (Bluhm et al. 2018)

Equation 4 Integrated meiofauna individuals m^{-2} (Bluhm et al. 2018)

Equation 5 Multiple linear regression model

List of abbreviations

IB	Inglefieldbukta
AGA	Agardhbukta
VMF	Van Mijenfjorden
PAL	Palanderbukta
WB	Wahlenbergfjorden
HTR	Hurtigruten
Chl *a*	Chlorophyll *a*
PCR	Polymerase chain reaction
CTD	Conductivity, temperature, density (depth)
SD	Standard deviation
dNTP	Deoxyribonucleotide triphosphate
DNA	Deoxyribonucleic acid
rRNA	Ribosomal ribonuclei acid
COI	Cytochrome oxidase c subunit 1
UNIS	The University Centre in Svalbard
$MgCl_2$	Magnesium chloride
HCl	Hydrochloric acid
mM	Millimolar
Rpm	Rounds per minute
ALB	Alkaline lysis buffer
NB	Neutralization buffer
SPRI	Solid-phase reversible immobilization

— intentionally left blank —

MASTER THESIS

Community composition, population structure and phylogeny of coastal sympagic meiofauna in eastern Svalbard

Magnus Heide Andreasen

Abstract Coastal sea ice communities constitute a highly vulnerable yet little investigated part of the Arctic ecosystem. A better understanding of the Arctic sea ice ecosystem will aid in more accurate predictions of the ecological response to current climate change. Sea ice communities comprise microalgae and meiofauna (20-500 μm) important to the existence and functioning of higher trophic levels. The response of sea ice-associated (sympagic) algae and meiofauna to current physical alterations in the Arctic will thus expectedly have ecosystem-wide consequences. Fundamental to the understanding of any ecosystem is knowledge on its taxa composition, species diversity and species functioning. This study investigated the community composition, population structure and phylogeny of coastal sympagic meiofauna in an unexplored region of eastern Svalbard in March and April 2018. Ice cores were extracted for sympagic and pelagic meiofauna, chlorophyll *a* and physical variables in Inglefieldbukta and Agardhbukta. Microscope photography was applied to explore the size, feeding and reproduction of polychaetes and nematodes. Further, molecular barcoding aided in identifying sympagic polychaetes and nematodes from three additional locations around Svalbard. Integrated sympagic meiofauna abundances ranged from 0 to 22 900 individuals m^{-2} with the most abundant and diverse communities occurring in April. Use of sea ice for overwintering, growth and reproduction was implied for nematodes, while polychaetes occurred only as feeding juveniles. Molecular analysis indicated the presence of two polychaete species not yet considered to be sympagic, *Melaenis loveni* and a *Spio* sp., and at least two nematode species not priorly described from Svalbard sea ice. The finding of *M. loveni* challenges the presumption of *Scolelepis squamata* as the resident sympagic polychaete in Svalbard. The nematodes collected in this study likely provide the first molecular evidence for *Theristus melnikovi* and possibly the first sign of an Arctic sympagic species within the genus *Halomonhystera*. The above findings suggest eastern Svalbard to be a particular interesting area to conduct more extensive studies on the poorly known sympagic meiofauna and their fate in a melting Arctic.

Keywords Arctic · Sea ice · Climate change · Nematodes · Polychaetes · Barcoding

Introduction

The Arctic Ocean constitutes an area of high scientific, political and socioeconomic interest owing to its rapid physical transformation. Most apparent is the rapid decrease of sea ice (Notz and Stroeve 2016; Stroeve and Notz 2018); yielding imminent opportunities for shipping (Dimitrios and Baxevani 2018), tourism (Dawson et al. 2016) and oil and gas exploration (ACIA 2004). The effects of decreasing sea ice on the relative abundance, life-history and diversity of Arctic biota are complex and little understood (Wassmann et al. 2011). It is evident that Arctic megafauna, e.g. polar bears (*Ursus maritimus*), walrus (*Odobenus rosmarus*) and ringed seal (*Pusa hispida*) are vital in ecosystem functioning and in the preservation of high-Arctic culture (George et al. 2004). However, 72 to 100% of polar bear diet is traceable to sympagic (= sea ice-associated) primary production (Brown et al. 2018). Investigating the lower sympagic trophic levels is thus a vital step in understanding the dynamics of the Arctic Ocean's ecosystem.

In sympagic communities, autotrophic protists, especially diatoms (*Bacillariophyceae*), together with bacteria make up the lowest trophic level, followed by metazoans mostly in the size range defining meiofauna; 20-500 µm (Bluhm et al. 2018). In Arctic sea ice, polychaete juveniles, nematodes, rotifers and ciliates are common inhabitants of the inner matrix of brine channels (Legendre et al. 1992; Gradinger 1999; Marquardt et al. 2011; Pitusi 2016). In addition, the interphase between sea ice and seawater is inhabited by ice amphipods, e.g. *Onismus nanseni* and *Apherusa glacialis*, and copepods of all life stages (Bradstreet and Cross 1982; Lønne and Gulliksen 1989; David et al. 2015, 2016, Kohlbach et al. 2016, 2017) with several other phyla represented although typically in low abundances (Werner 2005). The trophic dynamics of sympagic meiofauna remain largely unresolved. Repeated findings of low grazing pressure on sympagic algae (Gradinger 1999; Nozais et al. 2001; Michel et al. 2002; Gradinger et al. 2005) and occurrence of both carnivory, omnivory and cannibalism indicate that the sympagic ecosystem is highly complex (Kramer 2010). Sympagic meiofauna communities are structured by the age (Lønne and Gulliksen 1991a, b; Kiko et al. 2017), location (van Leeuwe et al. 2018) and type of sea ice, i.e. pack vs. fast ice (Marquardt et al. 2011) as well as connectivity with the pelagic and benthic realm. Hence, sympagic communities in shallow coastal areas exhibit a closer resemblance with benthic communities compared to sympagic communities overlying deep water (Bluhm et al. 2018). Distinct physical requirements exist in the matrix of brine channels inhabited by sympagic biota; temperatures below 40 °C and salinities fluctuating between 0 and above 100 (Ewert and Deming 2013). Moreover, biological processes; dispersal (Kiko et al. 2017) and competition (Krembs et al. 2000) shape sympagic communities at various spatial and temporal scales.

Logistic constrains associated with investigating sea ice systems limit studies of high temporal and spatial resolution, e.g. those examining life history patterns. While some sympagic meiofauna, autochthonous meiofauna, rely on sea ice throughout their entire life history, other, *inter alia* polychaete juveniles, utilize sea ice only temporarily; allochtonous meiofauna (Legendre et al. 1992; Thomas and Dieckmann 2009). In seasonal ice, sympagic communities consequently comprise allochtonous fauna that rely on annual incorporation into sea ice. The debate about to what extent sea ice colonization is coincidental or a matter of adaption is however still ongoing for some taxa (Spindler and Dieckmann 1986; Krembs et al. 2000; Chresten et al. 2016). Still, for highly motile taxa; nematodes, and polychaete juveniles, sea ice provides an attractive habitat periodically rich on algal and bacterial production (McConnell et al. 2012) supporting intentional colonization.

Polychaetes constitute a taxonomically and functionally diverse (Barnes and Fauchald 1979; Snelgrove 1997; Hutchings 1998) paraphyletic group with 14 000 recognized species (Rouse and Pleijel 2006). However, phylogeny of polychaetes remains unresolved (Rousset et al. 2007) largely owing to complications associated with identification (Bleidorn et al. 2003; Eklöf 2010). With molecular technology advances, the traditional belief of numerous polychaetes species being cosmopolitans has been challenged by continued findings of greater diversity (Bhaud and Petti 2001; Bhaud et al. 2006; Bleidorn et al. 2006; Scarpa et al. 2016; Hutchings and Kupriyanova 2018). Through identifying species-specific molecular sequences, 'barcodes', organisms can be identified without the need of morphological identification (Hebert et al. 2003; Blaxter 2004). In Antarctica, benthic meiofaunal diversity increased substantially when using barcoding despite reference data being lacking for most sequences (Fonseca et al. 2017). The finding of Fonseca et al. (2017) underlines the methodological prerequisite of establishment of high-quality sequences linked to voucher species accessible in public gene libraries, such as the Barcode of Life (Ratnasingham and Herbert 2007) and Genbank (Benson et al. 2013). Sympagic polychaete taxonomy still largely relies on morphological identification (McConnell et al. 2012) with *Scolelepis squamata* representing the only known sympagic polychaete (Carey 1985; Grainger et al. 1985).

Nematodes have, despite limited dispersal capacity, adapted to inhabit most environments, i.e. soils (Nicholas 1975), beaches (Hua et al. 2016), marine sediments (Fonseca et al. 2017), the pelagic realm (Tchesunov and Portnova 2015), multiple animal hosts as a parasite (Leung and Koprivnikar 2016), and sea ice (Tchesunov and Riemann 1995). Life histories of nematodes are highly diverse with longevity ranging between 3 days and 15 years (Gems and Riddle 2000), multiple reproductive strategies, i.e. ovipari and ovivipari (Gerlach and Schrage 1971), variable diets and flexible timing of egg cleavage (Chitwood and Murphy 1964). Romeyn and Bouwman (1983) identified nematodes' burrowing capacity, high tolerance to environmental stress and

diversification in buccal structure as characters explaining their dominance. Although often reported in a benthic context, nematodes frequently dominate sea ice communities too (Carey 1982; Grainger et al. 1985) with densities above 232.000 m^{-2} (Bluhm et al. 2018). At present, four nematodes are considered sympagic: *Theristus melnikovi* (Tchesunov 1986, *in Russian*), *Cryonema crassum*, *C. tenue* (Tchesunov and Riemann 1995) and *Hieminema obliquorum* (Riemann and Sime-Ngando 1997; Tchesunov and Portnova 2005). Their life cycles, however, remain conspicuous as they are yet to be registered in the benthic or pelagic realm (Tchesunov and Portnova 2003, 2005). In addition, three to four species within the *Monhysteridae* family remain unidentified from investigations in the White Sea (Tchesunov and Portnova 2003) and the Canadian Arctic (Riemann and Sime-Ngando 1997). A single *Halomonhystera glaciei* represents the only registration of nematodes in Antarctic sea ice (Blome and Riemann 1999). Sympagic nematode distribution and abundance is little known as expert taxonomist are required to distinguish morphological characteristics; sometimes at the scale beyond that of light microscopy (Coomans 2002; De Ley et al. 2005). However, as for polychaetes, molecular markers have proven useful in identification of nematodes (Avó et al. 2017; Fonseca et al. 2017). Still, phylogenetic analysis remains a challenging task for a cosmopolitan taxon with high genetic diversity within small spatial scales (Derycke et al. 2005, 2006). In 2017 (Avó et al. 2017), 1020 sequences existed for the 18S rRNA barcode (Bhadury et al. 2006; Creer et al. 2010; Porazinska et al. 2010) and 281 for the cytochrome c oxidase subunit I (COI) with no sympagic nematodes represented. While 18S rRNA remains the preferred barcode for nematodes, COI represents the most applied for polychaetes (Rice et al. 2008; Olson et al. 2009; Barroso et al. 2010; Nygren and Pleijel 2010). Based on the morphological complexity and incomplete sequence libraries, it is evident that sympagic nematode and polychaete diversity and phylogeny remains unresolved.

Phenetic plasticity, functional diversity and species richness determine ecosystem resilience (Oliver et al. 2015; Thomsen et al. 2019). Investigating coastal sympagic meiofauna communities' taxonomical diversity, phylogeny and respective life histories is thus vital in predicting the ecological implications of current physical alterations in the Arctic. Equally relevant, e.g. for incorporation into ecosystem models (Jin et al. 2006), is the establishment of baseline knowledge on coastal sympagic ecosystem community composition and their relation to the physical environment. Svalbard is of scientific interest due to the close physical resemblance of its coasts with those of other high-Arctic systems, i.e. Greenland (Madsen 1936; Petersen 1962) and Baffin Island (Ellis 1955; Ellis and Wilce 1961), as well as its well-established scientific and logistic facilities representing 45 nations (UNIS 2017). To date, most biological investigations have been conducted in western Svalbard (Kedra et al. 2013; Lowther et al. 2017; Bluhm et al. 2018; Daase et al. 2018)

and thus knowledge on marine biodiversity and community composition in eastern Svalbard is still poor (but see Szymelfenig et al. 1997; Schünemann 2004; Werner 2005)

This study represents the first effort to assess the composition of the coastal sympagic meiofauna community in eastern Svalbard. Length measurements on polychaetes and nematodes were applied to explore population structure. Finally, molecular analysis aided in investigating the diversity and phylogeny of polychaetes and nematodes based on samples from five locations around Svalbard.

Materials and methods

Field collection

Samples for sympagic meiofauna and chlorophyll *a* (hereafter Chl *a*), physical variables, length measurements and phylogeny were collected in Inglefieldbukta and Agardhbukta (Fig. 1) in spring 2018. In addition, samples for phylogenetic reference were collected in Wahlenbergfjorden and Palanderbukta in north-eastern Svalbard. Nematodes and polychaetes collected from Van Mijenfjorden in 2017 (c.f. Pitusi 2019) were also included to represent a temporally, spatially and physically distant reference group (Appendix 1). For a description of Wahlenbergfjorden, Palanderbukta and Van Mijenfjorden, see Appendix 2 and 3. Inglefieldbukta is situated at the joint mouth of the glaciers Inglefieldbreen and Nordsysselbreen and constitute the 2.5 km wide and long bay transitioning glacial and riverine runoff from west with Storfjorden to the east (Fig. 1).

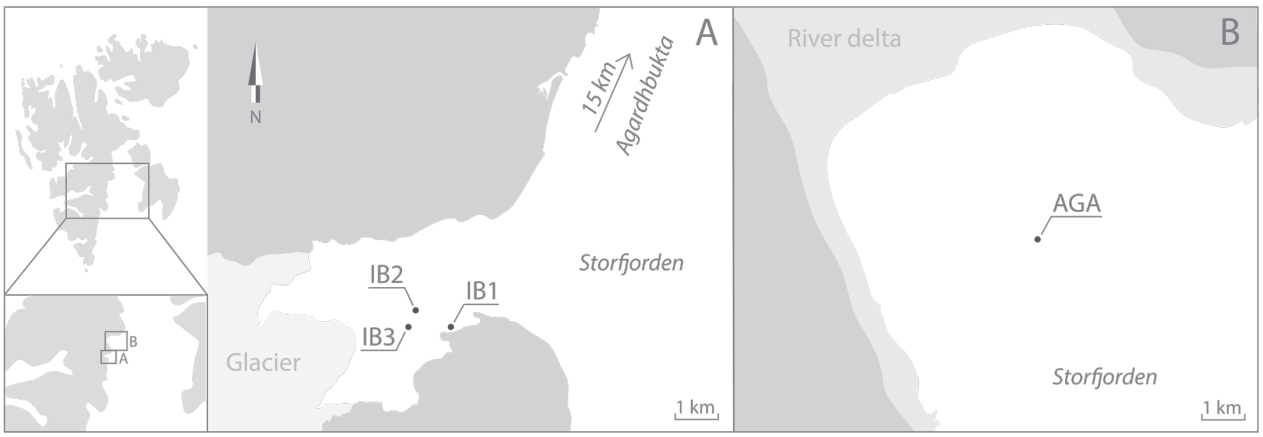

Figure 1. Sampling stations in Inglefieldbukta (A; IB) and Agardhbukta (B; AGA) in eastern Svalbard, Norway.

The first bathymetric data in Inglefieldbukta were collected as a part of this study. The depth transect indicated the presence of a basin with a sill depth of approximately 9 m towards east and

a maximum depth of 32 m closest to the glacial mouth. In Storfjorden, fast-ice cover is extensive during winter (see sea ice charts in Appendix 4) with sea ice production occurring mostly in polynyas northeast of Inglefieldbukta (Haarpaintner et al. 2001). Agardhbukta is situated 7 km north of Inglefieldbukta. Here, the valley Agardhdalen constitutes a large catchment area for runoff from several inland glaciers, rivers and streams, whose cumulative runoff terminates into the 8 km wide and 5 km long Agardhbukta. Hence, the two investigated sites differ in size and influence of glacial versus riverine runoff. In Inglefieldbukta, one shallow (4 m) and one deep (32 m) station was investigated in both March and April, whereas in Agardh only one station was investigated in April (AGA; 42 m). While the shallow station in Inglefieldbukta (IB1) was at the same location in March and April, the deep station was situated 200 meters apart. In March, the deep station (IB2) was ridge-free, whereas in April (IB3), the deep station had glacial ice incorporated into the sea ice.

The physical environment

To examine the physical environment of the sea ice, one core was extracted for temperature and another for salinity at each station. Cores extracted for temperature were measured (VWR Traceable Digital Thermometer) at the core's centre after drilling in 0.5 cm from below and at 1, 2, 3, 5 and 15 cm perpendicularly, continuing at 10 cm intervals to the top of the core. The salinity core was sectioned from 0-1, 1-2, 2-3, 3-10, 10-20 cm, continuing with 10 cm sections until the top of the core. Salinity sections were transferred into ziplock bags and thawed at room temperature for consequent analysis using a conductivity sensormeter (VWR Symphony SP90M5). Brine salinity (S_{brine}) and brine volume (V_{brine}) was calculated based on bulk ice salinity (S_{ice}) and ice temperature (T_{ice}) using the equations by Cox and Weeks (1983; Eq. 1 and 2).

$$S_{brine} = \frac{1000}{\left(1 - \frac{54.11}{T_{ice}}\right)} \qquad \text{Eq. 1}$$

$$V_{brine} = S_{ice}\left(0.0532 - \frac{4.919}{T_{ice}}\right) \qquad \text{Eq. 2}$$

For all extracted cores, snow was cleared in a 10 cm perimeter around the hole followed by measures of snow depth (average of three measurements), free-board and ice thickness. To assess the topology of the area surrounding the sampling stations, aerial photography (DJI Phantom 4 Advanced, DJI, China) was applied in April in both Agardhbukta and Inglefieldbukta (Appendix

5). Further, at all stations in both March and April, an underwater camera (GoPro HERO 4 Black, GoPro Inc., U.S.A.) was used to assess the sub-ice structure.

Chlorophyll *a*

At each station, ice algal biomass was determined by sampling three sea ice cores divided into sections as described above for salinity, although with further care taken to avoid irradiance and drainage. For every 1 cm of sea ice core, 100 ml of filtered sea water (0.7 µm) was added to the ziplock bags to avoid osmotic shock (Garrison and Buck 1986; Spindler and Dieckmann 1986) when slowly being thawed in darkness at +4 °C. Prior to filtration, each ice sections total volume was measured, and total Chl *a* obtained by pump-filtering samples in triplicates of 10 – 1120 ml using 0.7 µm Whatman GF/F glass fibre filters (Whatman, England). Pelagic Chl *a* biomass (phytoplankton biomass), was estimated by filtering 500 ml triplicate subsamples from Niskin bottle water samples at 3 m at IB2, at 1, 5 and 15 m at IB3 and in addition at 37 m at AGA. Total Chl *a* was stored in 10 ml 100% methanol in darkness for 24 hours at +4 °C (Holm-Hansen and Riemann 1978) and fluorescence were measured using an F10-AU Fluorometer (Turner Design, USA). Samples were diluted in 100% methanol when Chl *a* content exceeded maximum reading value. Two drops of 5% HCl were added to every sample to account for phaeopigments. Only Chl *a* values corrected for phaeopigments are included in this paper.

Sympagic meiofauna

As for Chl *a*, three sea ice cores were collected and processed per section (0-1, 1-2, 2-3, 3-10, 10-20 cm, continuing throughout the core in 10 cm sections) for examination of meiofauna communities. After slowly thawing sea ice samples in darkness at +4 °C, total sample volume was recorded and the sample was further filtered through a 20 µm sieve, counted, identified visually to lowest possible taxonomical level and photographed (Sony Handycam, SONY CO., U.S.A.) through a stereomicroscope (Leica Wild M3B, 1.6 – 11.5x magnification). Ciliates were only displayed when the quantification procedure followed that of the remaining groups; polychaetes, nematodes, trochophores, rotifers, eggs and unidentified (Fig. 4). All nematodes and polychaetes were isolated from samples and placed in individual Eppendorf tubes (1.5 mL, Eppendorf, Germany) containing 96% EtOH for subsequent phylogenetic analysis. All counts were converted into individuals per m^2 by averaging triplicates per section and integrating over the core. Only the lower 10 cm were included as described in Pitusi (2016) and corrected using the equation by Bluhm et

al. (2018), although with a lower ice-water density conversion factor (C; 0.93) considered suitable for first-year sea ice, following Timco and Frederking (1996) (Eq. 3). The abbreviations *h*, *n* and *V* refer to height of the core (cm), number of individuals in a core section and volume filtered (ml), respectively. To integrate the values, calculations followed Equation 4.

$$y = \frac{1000Chn}{V} \qquad \text{Eq. 3}$$

$$y_T = \sum_{i=0}^{N} y_i \qquad \text{Eq. 4}$$

The non-parametric Spearman rank correlation test (Spearman 1904) was applied to explore the relationships between sympagic meiofauna abundance and sympagic Chl *a* concentration as well as the relationship between biotic and abiotic variables.

Hydrography

To investigate the physics of the water column; conductivity, temperature, density and fluorescence was measured in the water column using a handheld CTD (SAIV A/S, Norway) and fluorometer from a hole within a 10-meter perimeter of the sea ice samples. Irradiance was measured from a separate hole using a LI-192 quantum sensor (LI-COR, Lincoln, USA) at 1-meter depth intervals. To avoid additional light pollution, the hole was covered in ice and snow before measurements.

Pelagic meiofauna

To examine the abundance of pelagic meiofauna, a 20 µm plankton net (HYDRO-BIOS, Germany) was hauled from the CTD hole and concentrated through a 20 µm sieve. At least two net samples were collected; one preserved in 70-80% ethanol and one in a 4% formalin-seawater solution buffered with hexamine. In Inglefieldbukta and Agardhbukta, vertical net hauls to maximum depth with a safety margin of 3 m from the bottom and up were sampled with a towing speed of 0.3-0.4 m s^{-1}. In the laboratory, fixative solution was removed by sieving the samples through a 20 µm sieve and rinsed with filtered sea water (0.7 µm Whatman GF/F glass fibre filters) for 30 minutes. The entire sample was counted using a stereomicroscope (Leica Wild M3B, 1.6 – 11.5x

magnification) and taxa identified to lowest possible taxonomical level. Copepodite stages were not distinguished as the dominating meiofauna, e.g. nematodes and polychaetes juveniles, were prioritized.

Length measurements

Polychaetes and nematodes isolated for phylogenetic analysis were manually length-measured in ImageJ (Schindelin et al. 2012; Rueden et al. 2017) based on individual stereomicroscope (Leica Wild M3B, 1.6 – 11.5x magnification) photographs (Sony Handycam HD, Sony Inc.). A multiple regression model (Frasier 2015) was applied to examine the response in length on date (March to May) and site (Van Mijenfjorden versus east coast stations Inglefieldbukta and Agardhbukta). To do so, model requirements, i.e. multivariate normality, homoscedasticity and absence of multicollinearity were met (Ralph 2015) and interannual length variation assumed neglectable compared to the seasonal variation investigated here. Selection, construction and testing of the model is summarized in Appendix 6.

DNA extraction, PCR and purification

DNA from polychaetes and nematodes was extracted using a commercial DNA extraction kit (Blood & Tissue Kit, QIAGEN). When DNA was not successfully isolated using the Blood & Tissue Kit, HotSHOT extraction was applied (Truett et al. 2000). To increase amplification success of polychaetes, two primer combinations were applied in amplifying polychaete COI DNA, while one was applied for nematodes (Appendix 7). A DreamTaq cycle (Thermo Fisher Scientific) was applied for both nematodes and polychaetes (95 °C – 5 min, 37 x (95 °C – 1 min, 54 °C – 1 min, 72 °C – 2 min), 4 °C – ∞). Following the recommendations of Leray and collaborators, a PlatiniumTaq touch down cycle (Korbie and Mattick 2008) was applied for polychaete individuals not yielding DNA through DreamTaq: 16 x (95 °C – 10 sec, 62 °C – 30 sec, (minus 2 °C for every 2nd cycle); 72 °C – 60 sec), 25 x (95 °C – 10 sec, 46 °C – 30 sec, 72 °C – 5 min, 4 °C – ∞ (Leray et al. 2013). The amplification was checked for success through gel electrophoresis, and the products were cleaned using HigherPurity™ solid-phase reversible immobilization (SPRI) cleaning (Canvax, Córdoba, Spain). Finally, cleaned products were Sanger sequenced (Sanger et al. 1977; GATC Biotech LightRun, Germany).

Bioinformatic analyses and phylogeny

Retrieved sequences were trimmed and checked for chimeras. Bad quality reads of a reading quality <10 constituted maximum five bases per sequence and were neutralized in Geneious Prime (Biomatters Ltd.). Consensus sequences were created only in instances where both complimentary sequences were of high quality. Sequences were compared to NCBI's database using BLAST. For polychaetes and nematodes, all available sequences of the most similar hits in BLAST were downloaded from NCBI's GenBank and aligned in MEGA7's MUSCLE software (Edgar 2004). Following alignment and end-trimming, trimmed sequences from this study were aligned. Lastly, outgroup sequences were aligned. For nematodes, *Diplolaimella dievengatensis* (Jacobs et al. 1990) was used as an outgroup following Tchesunov and Portnova (2015), while for polychaetes in Inglefieldbukta, a polychaete known to inhabit sea ice in Canada (Grainger et al. 1985), *Scolelepis squamata*, was chosen. For polychaetes isolated from sea ice in Van Mijenfjorden, another outgroup comprised by species of the *Bylgides* genera was chosen owing to the genetic dissimilarity to the polychaetes in Inglefieldbukta (GBIF.org; 2019; Norlinder et al. 2012). Any sequence yielding a length of less than 600 base pairs after alignment and trimming was discarded to retain robustness of the phylogenetic analysis. Consequently, the alignments were 632, 619 and 625 base pairs long for polychaetes in Inglefieldbukta and Van Mijenfjorden, and nematodes, respectively. Accession numbers for sequences included from reference studies are listed in Appendix 8.

To evaluate the most suitable evolutionary model supporting the phylogenetic analysis, MEGA7's model selection tool was applied. The Hasegawa-Kishino-Yano model (Hasegawa et al. 1985) assuming 59% of sites to be evolutionary invariable yielded the lowest Bayesian Information Criterion and was hence selected for the phylogenetic analysis of polychaetes. For nematodes, the Kimura 2-parameter model (Kimura 1980) assuming 45% of sites to be evolutionary invariable yielded the lowest Bayesian Information Criterion. To support the phylogenetic structure, maximum likelihood and maximum parsimony were applied in combination, both with 1000 replications, using MEGA7 (Kumar et al. 2016). For polychaetes in Van Mijenfjorden, maximum likelihood and neighbour joining were applied since maximum parsimony performs best in analyses on low genetic diversity.

Results

The physical environment

In Inglefieldbukta no glacial ice was observed in the nearby surroundings in March (radius = 100 meter), whereas in April, the deep sampling station was highly influenced by glacial ice visible both from above and below the sea ice (Fig. 1; Appendix 5). No glacial ice was visible within a perimeter of 1000 m in Agardhbukta. However, the snow was unevenly distributed (Table 1). Both snow depth and ice thickness increased throughout the sampling period, while freeboard was overall similar (1.4 to 4.5 cm), albeit with a negative average at IB3 (Table 1).

Table 1. Average (± SD) measures of physical parameters (cm) of the sea ice and snow in Inglefieldbukta (IB) and Agardhbukta (AGA) in Svalbard.

Date	Station	n	Snow depth	Ice thickness	Freeboard	Skeleton layer
March 22nd	IB1	8	2.8 ± 1.6	45.3 ± 1.8	3.2 ± 0.8	2.0 ± 1.5
March 23rd	IB2	8	9.9 ± 2.4	44.4 ± 1.8	1.4 ± 1.1	1.8 ± 0.8
April 15th	AGA	12	6.0 ± 4.3	62.0 ± 7.5	4.5 ± 1.9	0.9 ± 0.7
April 26th	IB1	9	13.9 ± 1.8	67.0 ± 1.0	3.1 ± 0.2	1.1 ± 0.3
April 27th	IB3	12	39.9 ± 1.0	86.5 ± 9.1	–0.7 ± 1.0	0.9 ± 0.3

Salinity, temperature, brine salinity and brine volume were investigated in vertical sea ice sections in Inglefieldbukta and Agardhbukta (Fig. 2). Salinity decreased the most within the lower 10 centimetres. In April, sea ice was thicker, and thus these profiles were longer. In Inglefieldbukta in late March and Agardhbukta in mid-April, a slight increase in salinity was observed in the uppermost sections, following a C-shape. Temperature profiles above 10 cm from the water varied markedly between March and April. In the lower 10 cm, however, temperature was similar across stations, sites and dates. As a direct function of sea ice temperature (Eq. 1), brine salinity displays a reverse profile with maxima occurring at the top. Conversely, brine volume decreased towards the top with the steepest decline in the lower 20 cm (Fig. 2).

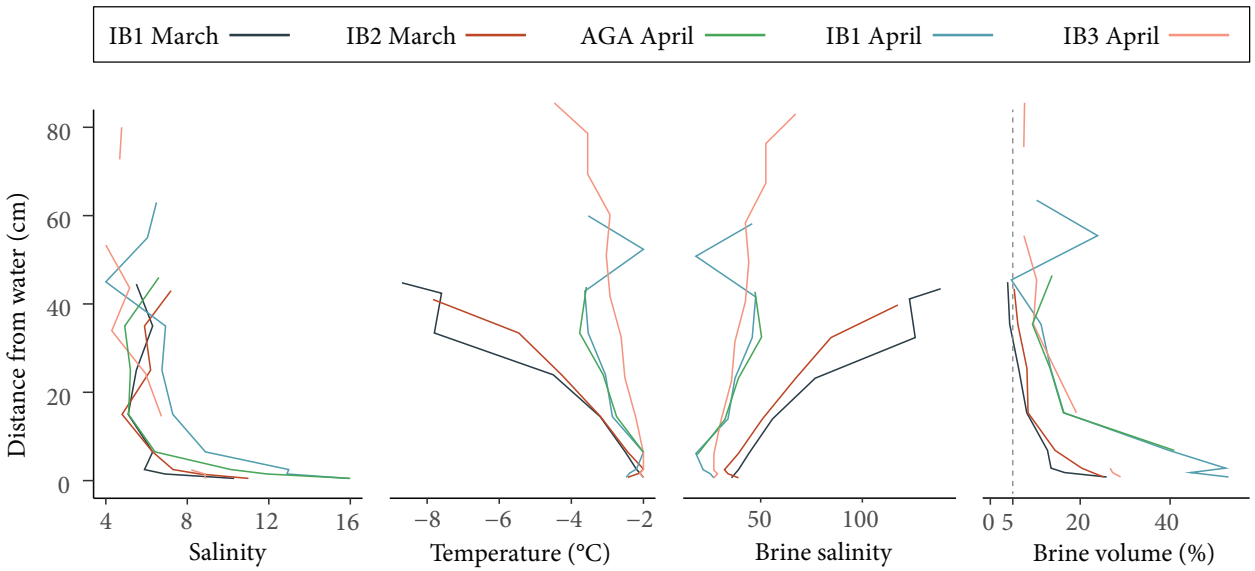

Figure 2. Vertical sea ice profiles of salinity, temperature, brine salinity and brine volume in Inglefieldbukta (shallow station: IB1 and deep stations: IB2, IB3) in March and April and Agardhbukta (AGA) in April 2018. The dashed line marks the 5% theoretical minima in brine volume for meiofauna to occur (Golden et al. 1998).

Although not visible from the extracted salinity cores or quantified otherwise, glacial ice was visible in >50% of cores extracted at IB3. No cores were solely constituted by glacial ice.

Hydrography and chlorophyll *a*

A CTD with a fluorometer attached yielded substantially different profiles in Inglefieldbukta in March (IB2) and April (IB3). However, the ~10 psu lower salinity and hence density in March is considered an instrument error. In both months, no pycnocline was present and fluorometry was low, i.e. <0.3 µg Chl *a* L^{-1}, although with a weak fluorometric increase from March to April (Fig. 3).

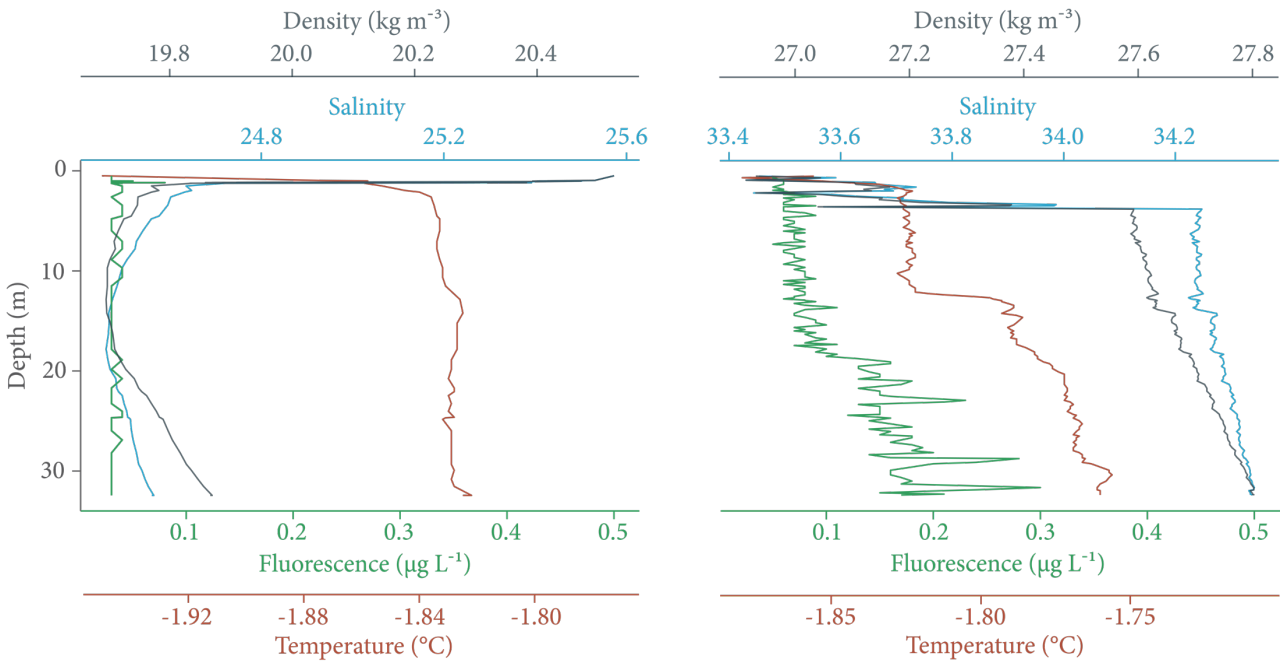

Figure 3. CTD and fluorescence profiles in Inglefieldbukta in March (left) and April (right) at deep stations IB2 and IB3, respectively.

Irradiance measured vertically from surface until lowest reading value resulted in maxima of 0.0138 and 0.0007 µmol s^{-1} m^{-2} for IB2 and IB3, respectively, followed by a similar extinction coefficient (k) of –0.08. In Agardhbukta, the maximum irradiance was 0.0080 µmol s^{-1} m^{-2} and the extinction coefficient –0.05.

In March, average integrated Chl *a* concentration in sea ice was low; 0.51 mg Chl *a* m^{-2} at IB1 and 0.07 mg Chl *a* m^{-2} at IB2. In April, the sea ice Chl *a* biomass had increased at IB1 (2.90 mg Chl *a* m^{-2}), while at IB3 in April, average concentration was 0.01 mg Chl *a* m^{-2}. Chl *a* peaked in Agardhbukta in April with 6.31 mg Chl *a* m^{-2}. In the water column at IB2 in March, the concentration of Chl *a* was on average 0.06 ± 0.06 µg Chl *a* L^{-1} at 3 m and at IB3 in April 0.08 ± 0.002 µg Chl *a* L^{-1} at 1, 5 and 15 meters. In Agardhbukta at 1, 5, 15 and 37 m, the Chl *a* concentration was low; on average 0.02 ± 0.006 µg Chl *a* L^{-1}. At all investigated stations, the sea ice algae communities were dominated by the pennate diatom *Nitzschia frigida* (Appendix 9). In Inglefieldbukta in March, the centric cold-water diatom *Melosira arctica* was observed in long chains (Appendix 10).

Sympagic meiofauna

Of the total 15 cores with each lower four sections (0-10 cm) investigated, 60% of the sections contained meiofauna yielding integrated abundances between 390 and 22 900 individuals m^{-2} in single cores. Integrated total and relative abundance of all registered taxa is displayed in Figure 4.

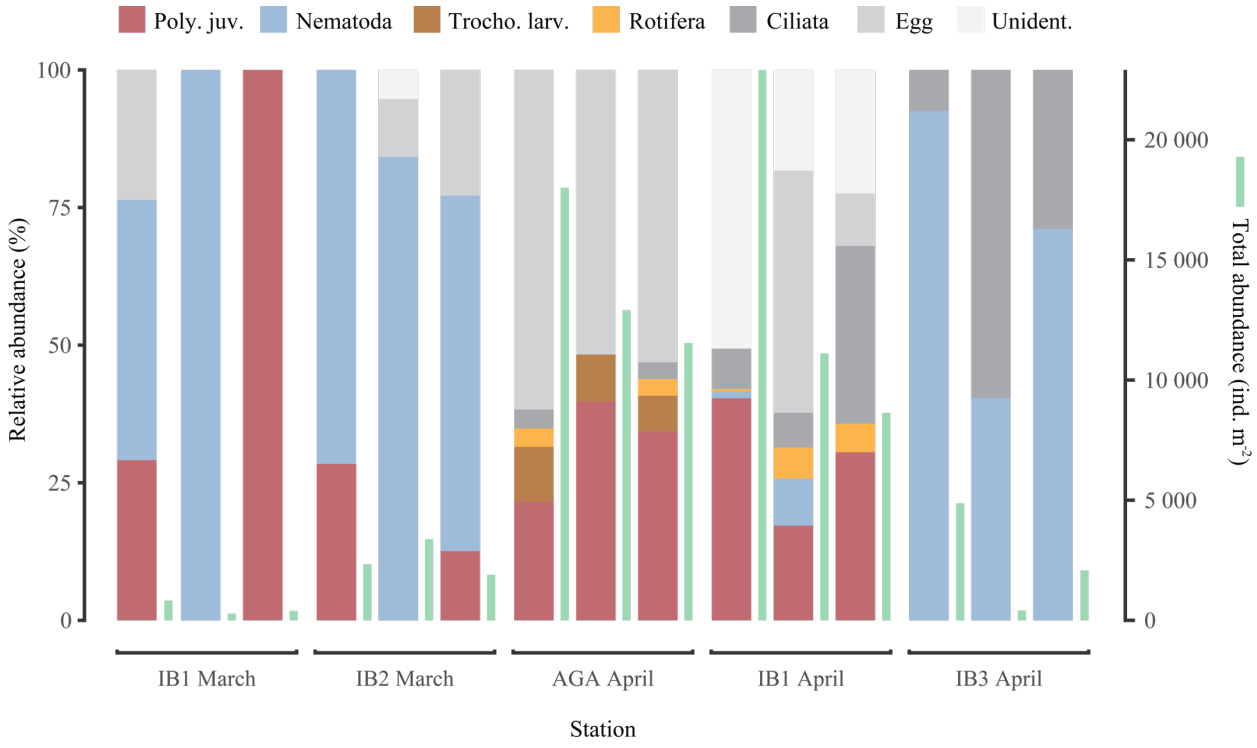

Figure 4. Integrated total and relative abundance of sympagic meiofauna in Inglefieldbukta (IB) and Agardhbukta (AGA) in eastern Svalbard, spring 2018. Poly. juv. = polychaete juvenile, Troch. larv. = trochophore larvae, Unident. = unidentified.

In March, especially at IB2, meiofauna communities were dominated by nematodes. However, in April, polychaetes, eggs and unidentified dominated IB1 while only nematodes and ciliates were registered at IB3. In Agardhbukta, eggs and polychaetes dominated followed by trochophores and rotifers. Ciliates were not quantified in March, but present at all stations in April. Eggs were registered at every station, except at station IB3.

Chlorophyll *a* and sympagic meiofauna

A significant positive relationship (*Spearman rank correlation*, ρ = 0.56, $p < 0.01$) was found between meiofauna abundance and Chl *a* concentration. However, the relationship was highly variable both within and between sites and sections (Fig. 5) and did not account for nematodes alone (p>0.1). Sympagic meiofauna abundance and Chl *a* concentration did not respond significantly to distance from sea ice-water interphase ($p > 0.1$), but both responded negatively to snow depth ($p < 0.05$).

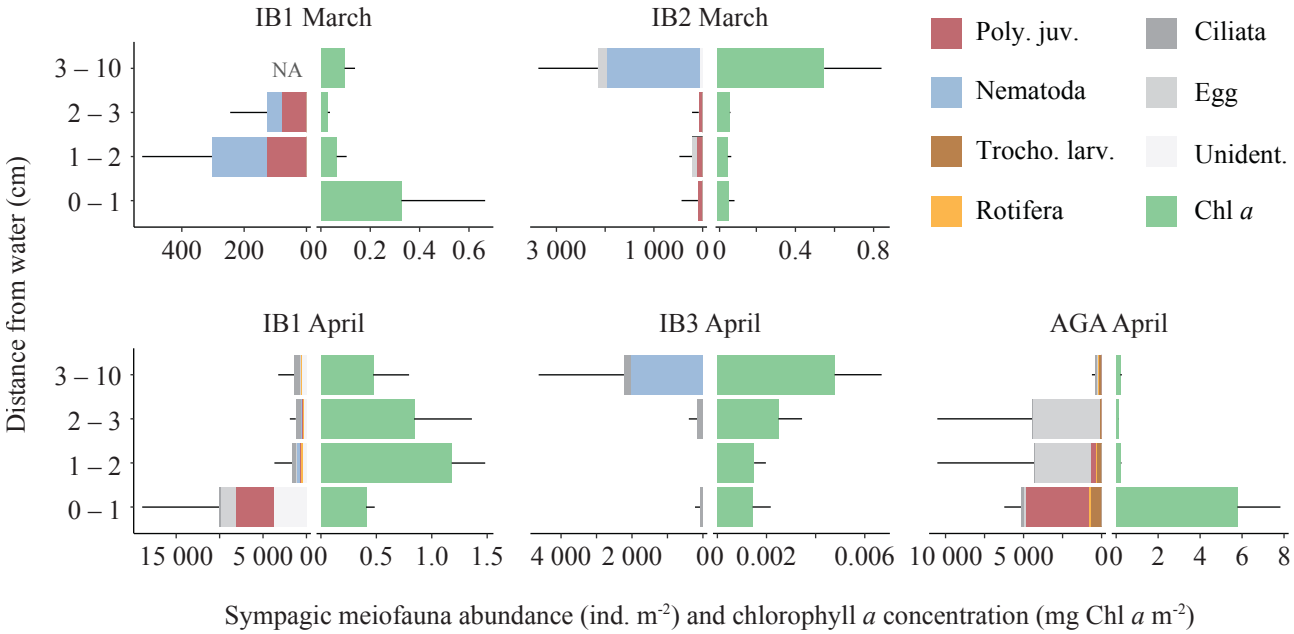

Figure 5. Sympagic meiofauna abundance (mean+SD; $n = 3$) and sympagic chlorophyll *a* (mean+SD; $n = 3$) in the lower 10 cm sections in Inglefieldbukta (IB1-3) and Agardhbukta (AGA) in eastern Svalbard, 2018. Poly. juv. = polychaete juvenile, Troch. larv. = trochophore larvae, Unident. = unidentified, Chl *a* = chlorophyll *a*. Note differences in scales.

Pelagic meiofauna

In Inglefieldbukta in March, 42 nematodes m^{-2} and one polychaete m^{-2} were registered in the water column at IB2, while in April, neither of the taxa were found despite two additional samples taken. Copepod nauplii dominated pelagic communities by accounting for 71% and 37% of the net microzooplankton community in March and April, respectively. In March, copepod nauplii, nematodes and copepods dominated, while in April, copepod nauplii, chaetognaths and copepods were

most numerous. The number of registered taxa increased from six to ten from March to April (Appendix 11).

Length measurements

Length of sympagic polychaetes found in sea ice increased significantly (ANCOVA; $p < 0.001$) throughout the season in both Van Mijenfjorden ($n = 60$), Inglefieldbukta ($n = 52$) and Agardhbukta ($n = 9$) with no significant difference in response between sites (ANCOVA test for comparison of regression line). The polychaetes in Van Mijenfjorden, however, were on average 96.1 µm larger than polychaetes at both east coast stations in March (ANCOVA; $p < 0.01$). All polychaetes in Inglefieldbukta were observed feeding when algae were present. The multiple linear regression model including date and site (VMF: 1; IB; 0) as predictors explained 27.4% of the variance in polychaete length (Eq. 5).

$$Length_{poly} = -126.7 + 5.6 \times day\ number + 96.1 \times site \qquad \text{Eq. 5}$$

Nematodes occurred in the sea ice in Inglefieldbukta at both shallow and deep stations in both March and April, but not in Agardhbukta. The length ranged from 266.9 (IB1, April) to 2242.1 µm (IB2, March). However, heteroscedasticity constrained modelling of nematodes. In Van Mijenfjorden, nematodes were on average 684.41 µm larger than nematodes in Inglefieldbukta with size generally decreasing in response to time at both sites. Still, the spread in size increased throughout the season with both juveniles (<1700 µm; Tchesunov and Riemann 1995) and adults occurring simultaneously in late April in both Van Mijenfjorden and Inglefieldbukta. In Inglefieldbukta (22nd of March 2018), 21 nematodes collected from the water column at IB2 were length measured. Compared to individuals measured in the overlying sea ice from the same day and station, the nematodes in the water were on average smaller (*two-sample t-test; $p<0.001$*) although the size range of the pelagic nematodes (638.7 – 1527.4 µm) were encompassed within that of the sympagic (603.6 – 2242.1 µm).

Phylogeny

Of the 63 polychaetes isolated from Inglefieldbukta for phylogenetic analysis, 10 polychaetes from IB1 in April were of good quality for further analysis, i.e. >620 base pairs, no gaps and high-quality reads. In addition, 25 sequences of the CMC strains from the Canadian Arctic (Carr et al.

2011) were aligned for reference. Maximum likelihood and maximum parsimony analyses revealed a similar clustering by outlining three clades indicated Clade 1, 2 and 3 in Figure 6. Six polychaetes of the CMC01 strain constituted Clade 1, while Clade 3 was constituted by 10 polychaetes of the CMC03 strain. The 10 polychaetes analysed in this study all grouped with the CMC02 strain, together constituting Clade 2 (Fig. 6).

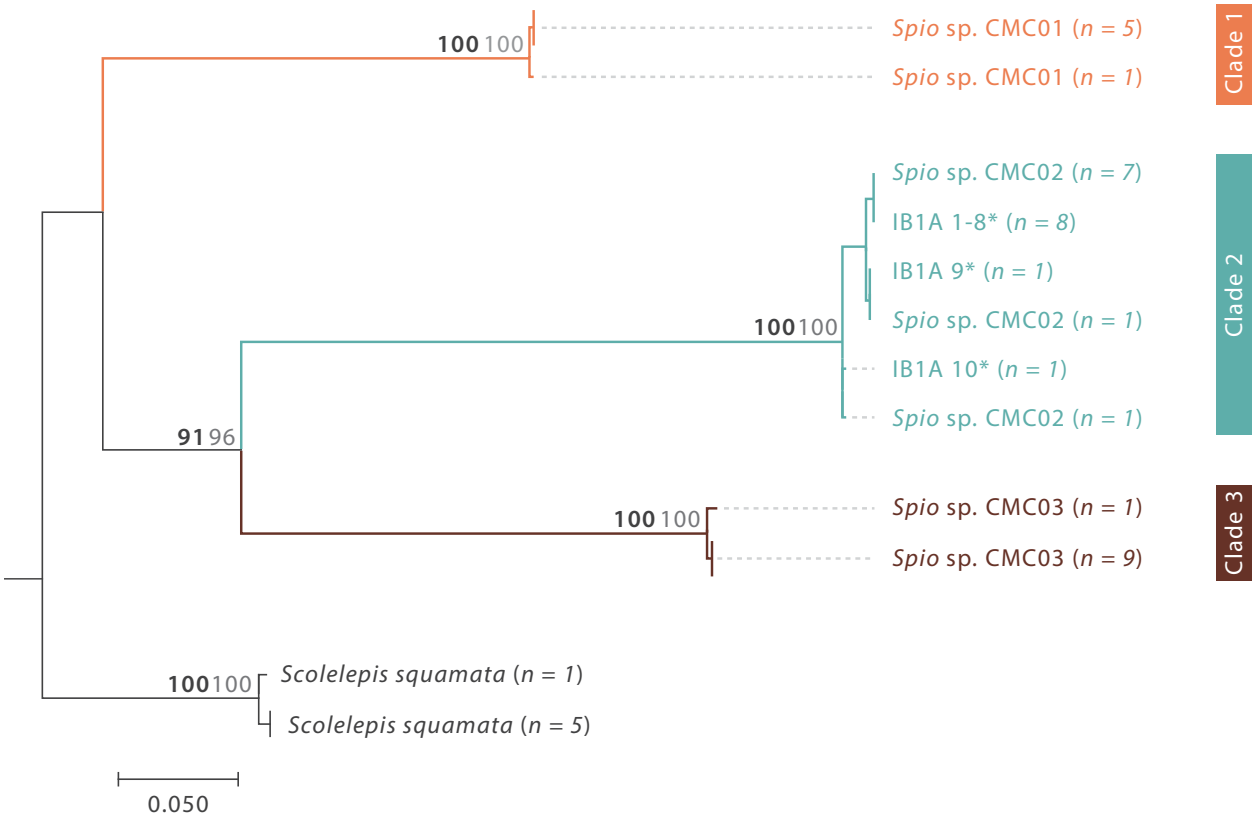

Figure 6. Phylogenetic tree based on maximum likelihood (bold bootstrap values) and maximum parsimony (grey bootstrap values) on 10 polychaetes from Inglefieldbukta in April and 25 polychaetes from the Canadian Arctic. Accession numbers are available in Appendix 8 and reference names in Appendix 12. *Sequences from this study.

Polychaetes isolated from Van Mijenfjorden in 2017 (*n = 13*) yielded three high quality sequences all genetically distant from polychaetes isolated from Inglefieldbukta. Hence, a separate molecular analysis including taxa of higher genetic similarity was done based on polychaete phylogeny summarized in the Global Biodiversity Information Facility (GBIF.org; 2019). Sequences belonging to neighbouring genera were thus identified (Appendix 8) and included in the analysis (Fig. 7).

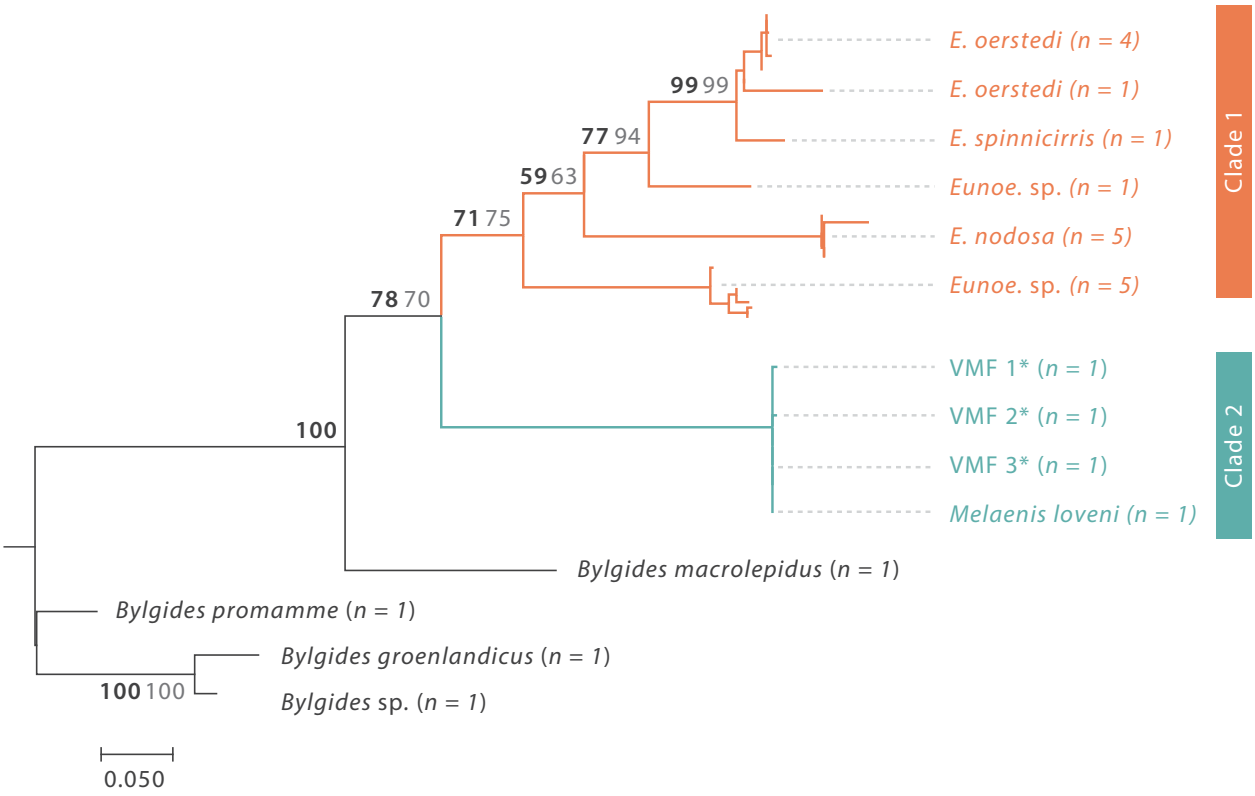

Figure 7. Phylogenetic tree based on maximum likelihood (bold bootstrap values) and neighbour joining (grey bootstrap values) on three polychaetes from Van Mijenfjorden April 2017 and 18 reference sequences mostly from the Canadian Arctic, Chukchi Sea and Svalbard. Accession numbers are available in Appendix 8 and reference names in Appendix 12. *Analysed in this study with sequences from Pitusi et al. (2019).

All polychaetes from Van Mijenfjorden places within Clade 2 together with a *Melaenis loveni* (Malmgren 1865) isolated from Svalbard waters, while Clade 1 is constituted by *Eunoe* spp. (Malmgren 1865).

Nematodes from IB1 (*n = 1*) and IB2 (*n = 6*) in March, Wahlenbergfjorden (WB) in May (*n = 2*) and Palanderbukta (PAL) in June (*n = 2*) yielded high quality sequences for phylogenetic analysis. Combined with sequences from Van Mijenfjorden (*n = 43*; Pitusi 2019), the Håkon Mosby Mud Volcano (*n = 5;* HMMV; Van Campenhout et al. 2014) and the west coast of the Netherlands (*n = 16*; Van Campenhout et al. 2014), maximum likelihood and maximum parsimony revealed similar phylogenetic clustering (Fig. 8). The included voucher sequences from HMMV and the Netherlands represent, to my knowledge, the accessible high-quality sequences on the *Halomonhystera* sp. 18S rRNA barcode in GenBank.

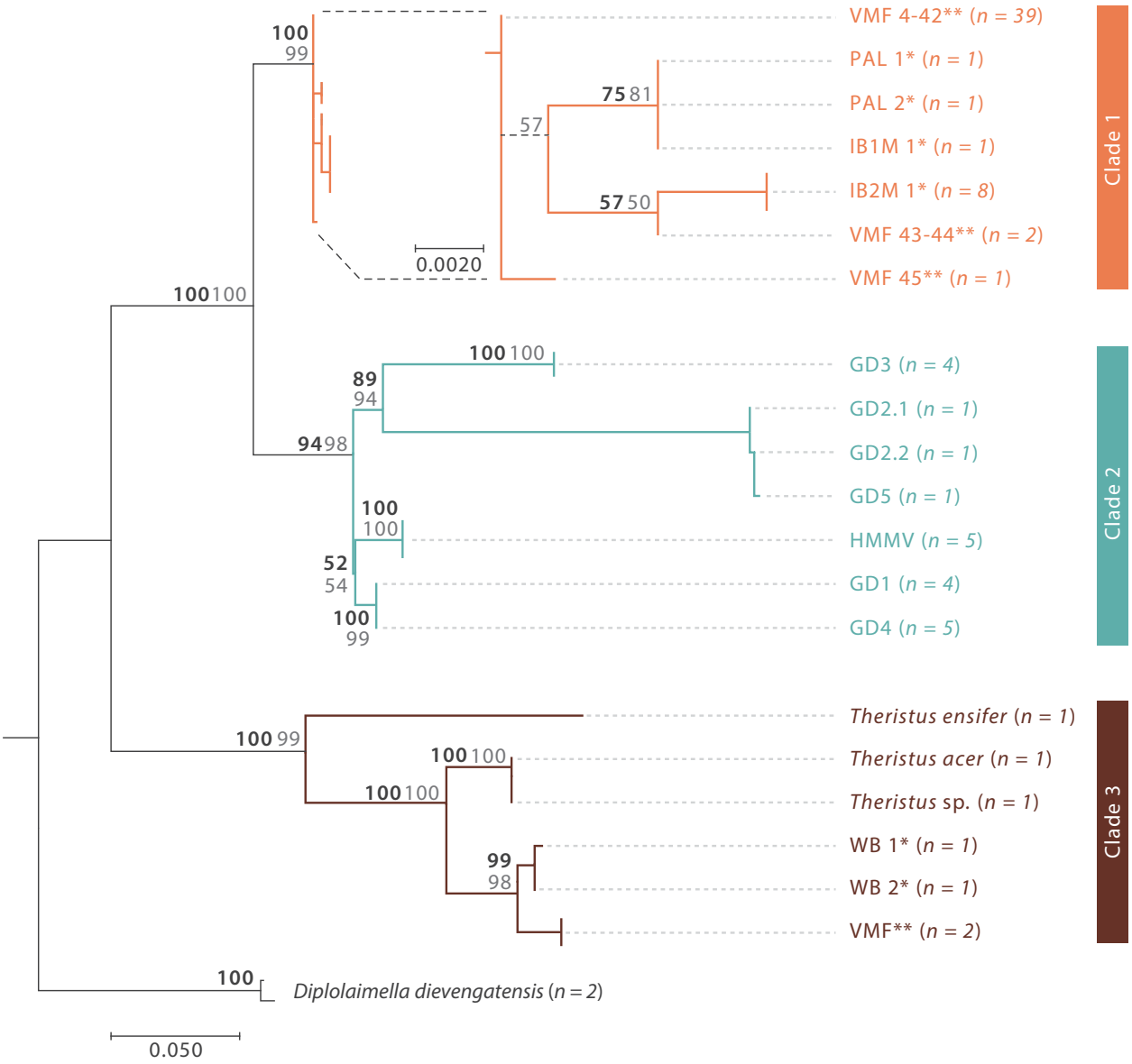

Figure 8. Phylogenetic tree based on maximum likelihood (bold bootstrap values) and maximum parsimony (grey bootstrap values) on seven nematodes from Inglefieldbukta (IB1-2), two from Palanderbukta (PAL), 44 from Van Mijenfjorden (VMF), 20 from the Netherlands (GD1-5; *Theristus*) and five from the Håkon Mosby Mud Volcano (HMMV). Accession numbers are available in Appendix 8 and reference names in Appendix 12. * Sequences from this study, ** Sequences from Pitusi (2019).

Three clades can be distinguished: Clade 1, 2 and 3. Clade 1 is constituted solely by individuals isolated from sea ice (IB1, IB2, PAL and VMF), while Clade 2 displays *Halomonhystera disjuncta* sequences isolated from sediments from the Netherlands (GD1-5) and Håkon Mosby Mud volcano (HMMV). Clade 3 is more distant to clade 1 and 2 and has a deeper branching containing a combination of sequences obtained from WB and VMF related to *Theristus* spp.

Discussion

The aim of this study was to determine the community composition of coastal sympagic meiofauna in eastern Svalbard. Further, the population structure of sympagic polychaetes and nematodes was examined based on registrations of eggs, concurrent sampling of the pelagic realm and length measurements with reference to sympagic communities in Van Mijenfjorden. To investigate the diversity and phylogeny of polychaetes and nematodes, molecular barcoding was applied. We found coastal sympagic communities in March constituted by coexisting polychaete juveniles and nematodes at low overall abundances, i.e. ≤626 ind. m^{-2}. In April, the sympagic communities were characterized by greater abundances, low coexistence of the two dominating phyla and the addition of trochophore larvae, rotifers and numerous eggs. Statistically significant increases in size and observations of feeding polychaetes implied that polychaete juveniles used the sympagic realm as a feeding ground, supporting earlier findings by Gradinger et al. (2009). Initial size increments, molecularly confirmed presence of eggs and later simultaneous occurrences of both adult and juvenile nematodes support that nematodes both feed, reproduce and raise juveniles inside the sea ice throughout the spring. While the habitat use appeared similar between polychaetes in Inglefieldbukta and Van Mijenfjorden, the species are seemingly different. Hence, at least one species within the genus *Spio* inhabits the east coast, while *Melaenis loveni* inhabits the west coast. Similarly, size patterns of nematodes in Inglefieldbukta and Van Mijenfjorden resembled each other despite having at least two species in Van Mijenfjorden and one species in Inglefieldbukta.

Community composition

Polychaetes and nematodes dominated the coastal sympagic community in Inglefieldbukta in March, albeit at relatively low abundances; 272-626 ind. m^{-2}. Contrary to expectations, little difference was observed in abundance and taxa composition between the shallow (4 m; IB1) and deep (32 m; IB2/3) station in March. From March to April, total abundance increased from 8 635 to 22 903 ind. m^{-2} at IB1, while the deep station (IB2) only increased slightly in abundance from March to April (IB3). Interestingly, Agardhbukta resembled the community of IB1, both with regards to abundance and community composition, but not IB3. Together, this underlines the substantial compositional variation typically observed within small spatial scales in sympagic meiofauna communities (Bluhm et al. 2018). The differences in depth (4 m versus 42 m), distance (15 km) and terrestrial input (glacier front versus river valley) encompassed here are likely too narrow to

explain the observed variation. Snow depth at IB3 was 39.9±1.0 cm; more than twice the thickness of both IB1 and AGA in April. Consequently, under-ice irradiance at IB3, 0.0007 µmol s^{-1} m^{-2}, was one order of magnitude lower than at the adjacent stations. Hence, variation in snow depth and the associated irradiance and Chl *a* might explain the observed community variation, i.e. a polychaete-dominated community at IB1 and AGA in April and a community dominated by nematodes and ciliates at IB3 in April. The availability of algae, here expressed as Chl *a*, shape sympagic meiofauna communities (Gradinger 1999; Schünemannn and Werner 2005) but is in turn rarely influenced by meiofaunal grazing (Gradinger 1999; Nozais et al. 2001; Michel et al. 2002; Gradinger et al. 2005). Still, polychaete abundance responded positively to the concentration of Chl *a*, while nematodes did not. Hence, only ciliates and nematodes were registered at IB3 where integrated Chl *a* was 0.01 mg Chl *a* m^{-2}. By being bacterivorous, nematodes and ciliates do not depend on algae-based energy (Tchesunov and Riemann 1995; Kramer 2010) as it is implied from the simultaneous relatively high nematode and ciliate abundance and low Chl *a* concentration at the uppermost section at IB2 and IB3 (Fig. 5). The absence of algae likely influences sympagic nematodes and ciliates indirectly by not supporting polychaete juveniles and hereby increase substrate availability and further directly by not competing with bacteria for inorganic nutrients (Appendix 13). Nematodes and ciliates are consequently potential important ecosystem components in coastal sympagic ecosystems where sympagic algae biomass is limited by low irradiance.

The presence of glacial ice inside the sea ice at the deep station in Inglefieldbukta in April (IB3; Appendix 5) provides an additional explanation for the low diversity and abundance of sympagic meiofauna here. Albeit not covered by salinity measurements herein, a lower brine volume is expected with the lower salinities of glacial ice (Golden et al. 1998; Krembs et al. 2000; Burton et al. 2018); consequently supressing the colonization and succession of sympagic biota.

A greater taxonomical richness and lower abundance was observed among the pelagic meiofauna at the deep stations with six and ten taxonomical groups in March (IB2) and April (IB3), compared to 4 and 6 in the sea ice, respectively. The finding of lower abundance of pelagic meiofauna are well in line with the concurrent low concentration of pelagic Chl *a* and follow findings in Storfjorden, north of Svalbard (Schünemann 2004) and in the Baltic Sea (Meiners et al. 2002). The lower diversity in the sympagic realm, compared to the pelagic realm, is likely a result of the strong selection for small, morphologically plastic taxa that can cope with the distinct physiochemistry of brine channels (Krembs et al. 2000). Only nematodes in March were simultaneously present in the sympagic and pelagic realm; indicating a habitat specificity for the investigated

meiofauna throughout March and April. The ability to thrive in both realms likely increases the fitness and resilience of sympagic nematodes.

Diversity of sympagic polychaetes and nematodes

It is still unclear which and how many polychaete and nematode species inhabit the sea ice in Svalbard. Molecular analyses in this study show the presence of at least two polychaete species; *Melaenis loveni* in Van Mijenfjorden and at least one species within the genus *Spio* in Inglefieldbukta. Both are, to my knowledge, new to the register of polychaetes inhabiting sea ice and challenge the presumption of *Scolelepis squamata* as the sole sea ice inhabitant in Svalbard. *M. loveni* is not new to the polychaete literature in Svalbard but has only been registered from the benthic environment, most recently by Norlinder et al. (2012) and initially by Wirén (1883) in Van Mijenfjorden during the Vega Expedition (1878-1879). *Spio* species have been described in the Arctic as early as 1776 (Müller 1776) and later by Schneider in 1977 (see Blum and Fong 2016). The sequences representing the *Spio* genera in this study originate from the Canadian Arctic (Carr et al. 2011) and represent the most genetically similar voucher genus available in GenBank (Benson et al. 2013). Expert taxonomists are required to establish voucher species for the polychaetes analysed here. While a pan-Arctic distribution is known for several meiofauna (Carr et al. 2011; Bluhm et al. 2018), it remains unknown if the same is true at the species level. It is thus intriguing to clarify the genetic similarity between the polychaetes collected in Svalbard and in Canada.

The sympagic nematodes analysed in this study constitute the first evidence of the sympagic nematode diversity in sea ice in Inglefieldbukta, Palanderbukta and Wahlenbergfjorden. Molecular analyses implied the presence of at least two species within separate genera; *Theristus* and another yet unknown genus with up to several species closely related to *Halomonhystera disjuncta*. *Theristus melnikovi* is known from sea ice in the Fram Strait, Laptev Sea and the Central Arctic Ocean (Tchesunov and Riemann 1995) but has not priorly been described for Svalbard. Here, a *Theristus* sp. occurred in Van Mijenfjorden in April ($n = 2$) and in Wahlenbergfjorden in May ($n = 2$); possibly adding to *T. melnikovi*'s apparent pan-Arctic distribution. Sea ice cover in Van Mijenfjorden and Wahlenbergfjorden is seasonal. Further, especially in Van Mijenfjorden, connectivity with external sea ice communities is scarce. Therefore, the presumed finding of T. *melnikovi* in Van Mijenfjorden and Wahlenbergfjorden indicate a sympago-benthic life strategy. Occurrences of *T. melnikovi* inside sea ice over deep water (1000-3000 m) in the Central Arctic Ocean and Fram Strait (Tchesunov and Riemann 1995) can be explained by dispersal from neighboring

seed communities as has been suggested for sympagic algae (Kauko et al. 2018). While not identified to species level, nematodes within the *Theristus* genus have been observed in the benthos in the Laptev sea at depths from 65 m (Vanaverbeke et al. 1997). Hence, the Laptev Sea shelf provides shallow depths and polynyas potentially suitable for sea ice colonization and subsequent transpolar drift (Krumpen et al. 2019).

The unknown nematode genus' occurrence in both Palanderbukta, Inglefieldbukta and Van Mijenfjorden imply that at least two species coexist in the coastal sympagic communities in Svalbard. The sample size presented here is likely too scarce to cover the diversity of the respective sampling sites but provides a baseline for further sympagic meiofauna diversity studies in eastern Svalbard. Appendix 14 visually summarizes registrations of the polychaetes and nematodes discussed here.

Further prospects

Polychaetes and nematodes remain among the dominating meiofauna in coastal sympagic ecosystems in the Arctic (Kern and Carey 1983; Grainger et al. 1985; Gradinger et al. 2009; Marquardt et al. 2011). It is therefore fundamental to establish a record of their diversity, distribution and ecosystem function if we are to understand their ecological significance in Arctic coastal ecosystems. However, an extensive collection of voucher species created through close collaboration between molecular biologist and taxonomist is required followed by novel metagenetic approaches. This will aid in making currently challenging ecological questions more easily accessible, possibly through ecosystem-wide models (Zhang et al. 2010). To elucidate the life history of sympagic nematodes, future research should prioritize concurrent sampling of the pelagic and benthic realm when investigating sympagic nematodes. Greater dependency of the sympagic realm will likely result in greater ramifications for both higher and lower tropic level, following the current decline in sea ice extent. Hence, knowledge on habitat use and timing will aid in understanding and predicting the ecological response of sympagic nematodes in future climate scenarios. Further, exploring the generality of the influence of glacial ice incorporation, questioned in this study, can become useful when investigating coastal areas prone to glacial ice.

This study supports the use of Svalbard as a model area (CAFF 2017) with special emphasis on the eastern region investigated herein. The climate of the east coast resembles that of the more inaccessible high-Arctic; as underlined by the finding of the high-Arctic multiyear sea ice indicator species *Melosira arctica* in this study (Józef Wiktor, *pers. communication*). *M. arctica* relies on stability and is hence most prominent at the inner sections of ice sheets (Poulin and Michel 2014). Therefore, protected bays like Inglefieldbukta expectedly best resemble its high-Arctic habitat.

Conclusion

This paper provided insight into the community composition, population structure and phylogeny of coastal sympagic meiofauna in eastern Svalbard. Communities in March were lowest in abundance, i.e. ≤626 ind. m^{-2}, and comprised polychaete juveniles, nematodes and nematode eggs. In Inglefield in April, taxonomic diversity, polychaete juvenile dominance and total sympagic meiofauna abundance increased at the shallow station reaching abundances up to 22 900 ind. m^{-2}. The adjacent deep station comprised nematodes and ciliates. Snow depth and glacial ice most likely explains the observed variation in community composition between stations and dates. Observations of nematode size increments, molecular identification of nematode eggs and the subsequent presence of nematode juveniles imply that nematodes utilize the sympagic realm to feed, reproduce and raise juveniles. The presence of long chains of *Melosira arctica* confirms the relevance of the high-Arctic environment of eastern Svalbard as a model area for monitoring the response of sympagic ecosystems to diminishing sea ice. Finally, the addition of at least two meiofauna species new to sympagic literature implies that numerous discoveries await in eastern Svalbard for sympagic ecosystem research.

References

ACIA (2004) ACIA, Impacts of a Warming Arctic: Arctic Climate Impact Assessment

Allgén CA (1929) Südschwedische Marine Nematoden. Göteborgs K Vetens- och Vitterh Samh Handl 2:1–40

Avó AP, Daniell TJ, Neilson R, et al. (2017) DNA Barcoding and Morphological Identification of Benthic Nematodes Assemblages of Estuarine Intertidal Sediments: Advances in Molecular Tools for Biodiversity Assessment. Front Mar Sci 4. doi: 10.3389/fmars.2017.00066

Barnes M, Fauchald K (1979) The Diet of Worms: a Study of Polychaete Feeding Guilds. Ocean Mar Biol Ann Rev 17:193–284

Barroso R, Klautau M, Solé-Cava AM, Paiva PC (2010) *Eurythoe complanata* (Polychaeta: *Amphinomidae*), the 'cosmopolitan' fireworm, consists of at least three cryptic species. Mar Biol 157:69–80

Benson DA, Cavanaugh M, Clark K, et al (2013) GenBank. Nucleic Acids Res 41:D36–D42. doi: 10.1093/nar/gks1195

Bhadury P, Austen MC, Bilton DT, et al. (2006) Development and evaluation of a DNA-barcoding

approach for the rapid identification of nematodes. Mar Ecol Prog Ser 320:1–9

Bhaud M, Koh B-S, Martín D (2006) New systematic results based on chaetal hard structures in *Mesochaetopterus* (Polychaeta). Sci Mar 70:35–44

Bhaud MR, Petti MAV (2001) *Spiochaetopterus nonatoi*, a new species of *Chaetopteridae* (Polychaeta) from Brazil: biogeographical consequences. J Mar Biol Assoc United Kingdom 81:225–234

Blaxter ML (2004) The promise of a DNA taxonomy. Philos Trans R Soc London Ser B Biol Sci 359:669–679

Bleidorn C, Podsiadlowski L, Bartolomaeus T (2006) The complete mitochondrial genome of the orbiniid polychaete *Orbinia latreillii* (Annelida, *Orbiniidae*) – A novel gene order for Annelida and implications for annelid phylogeny. Gene 370:96–103. doi: https://doi.org/10.1016/j.gene.2005.11.018

Bleidorn C, Vogt L, Bartolomaeus T (2003) New insights into polychaete phylogeny (Annelida) inferred from 18S rDNA sequences. Mol Phylogenet Evol 29:279–288

Blome D, Riemann F (1999) Antarctic sea ice nematodes, with description of *Geomonystera glaciei* sp. n. (*Monhysteridae*). Mitt hamb zool Mus Inst 96:15–20

Bluhm BA, Hop H, Vihtakari M, et al. (2018) Sea ice meiofauna distribution on local to pan-Arctic scales. Ecol Evol 8:2350–2364. doi: 10.1002/ece3.3797

Blum S, Fong J (2016) CAS Invertebrate Zoology (IZ). GBIF.org. Accessed 27 May 2019

Bradstreet MSW, Cross WE (1982) Trophic Relationships at High Arctic Ice Edges. Arctic 35:1–12

Brown TA, Galicia MP, Thiemann GW, et al. (2018) High contributions of sea ice derived carbon in polar bear (*Ursus maritimus*) tissue. PLoS One 1–13

Burton JC, Amundson JM, Cassotto R, et al. (2018) Quantifying flow and stress in ice mélange, the world's largest granular material. PNAS 115:5105–5110. doi: 10.1073/pnas.1715136115

CAFF (2017) State of the Arctic Marine Biodiversity Report

Carey AG (1985) Marine ice fauna: Arctic In: Horner RA (ed), Sea ice biota. CRC Press 173–190

Carey AG (1982) Arctic Sea Ice Fauna1 Assemblage: First Approach Meiofauna. Mar Ecol 8:1–8

Carr CM, Hardy SM, Brown TM, et al. (2011) A Tri-Oceanic Perspective: DNA Barcoding Reveals Geographic Structure and Cryptic Diversity in Canadian Polychaetes. 6. doi: 10.1371/journal.pone.0022232

Chitwood BG, Murphy DG (1964) Observations on two marine monhysterids: their classification, cultivation, and behavior. Trans Am Microsc Soc 83:311–329

Chresten L, Hawes LI, Holtegaard M, Sorrell BK (2016) Is colonization of sea ice by diatoms facilitated by increased surface roughness in growing ice crystals? Polar Biol. doi: 10.1007/s00300-016-1981-3

Coomans A (2002) Present status and future of nematode systematics. Nematology 4:573–582

Creer S, Fonseca VG, Porazinska DL, et al. (2010) Ultrasequencing of the meiofaunal biosphere: practice, pitfalls and promises. Mol Ecol 19:4–20

Daase M, Kosobokova K, KS L, et al. (2018) New insights into the biology of *Calanus* spp. (Copepoda) males in the Arctic. Mar Ecol Prog Ser 607:53–69

David C, Lange B, Krumpen T, et al. (2016) Under-ice distribution of polar cod *Boreogadus saida* in the central Arctic Ocean and their association with sea-ice habitat properties. Polar Biol 39:981–994. doi: 10.1007/s00300-015-1774-0

David C, Lange B, Rabe B, Flores H (2015) Community structure of under-ice fauna in the Eurasian central Arctic Ocean in relation to environmental properties of sea-ice habitats. Mar Ecol Prog Ser 522:15–32

Dawson J, Stewart EJ, Johnston ME, et al. (2016) Identifying and evaluating adaptation strategies for cruise tourism in Arctic Canada in Arctic Canada. J Sustain Tour 9582. doi: 10.1080/09669582.2015.1125358

De Ley P, De Ley IT, Morris K, et al. (2005) An integrated approach to fast and informative morphological vouchering of nematodes for applications in molecular barcoding. Philos Trans R Soc B Biol Sci 360:1945–1958

Derycke S, Backeljau T, Vlaeminck C, et al. (2006) Seasonal dynamics of population genetic structure in cryptic taxa of the P*ellioditis marina* complex (Nematoda: Rhabditida). Genetica 128:307–321

Derycke S, Remerie T, Vierstraete A, et al. (2005) Mitochondrial DNA variation and cryptic speciation within the free-living marine nematode *Pellioditis marina*. Mar Ecol Prog Ser 300:91–103

Dimitrios D, Baxevani E (2018) The Future of Arctic Shipping Business and the Positive Influence of the International Code for Ships Operating in Polar Waters. Journal Ocean Technol

Edgar RC (2004) MUSCLE: a multiple sequence alignment method with reduced time and space complexity. BMC Bioinformatics 5:113

Eklöf J (2010) Taxonomy and phylogeny of polychaetes. Department of Zoology; Zoologiska institutionen

Ellis D V (1955) Some observations on the shore fauna of Baffin Island. Arctic 8:224–236

Ellis D V, Wilce RT (1961) Arctic and subarctic examples of intertidal zonation. Arctic 14:224–

235

Ewert M, Deming JW (2013) Sea Ice Microorganisms: Environmental Constraints and Extracellular Responses. Biology (Basel) 603–628. doi: 10.3390/biology2020603

Flink A, Noormets R, Fransner O, Hogan K (2014) Observations and implications of submarine landforms in Wahlenbergfjorden, Eastern Svalbard

Fonseca VG, Sinniger F, Gaspar JM, et al. (2017) Revealing higher than expected meiofaunal diversity in Antarctic sediments: A metabarcoding approach. Sci Rep 7:1–11. doi: 10.1038/s41598-017-06687-x

Frasier TR (2015) A note on the use of multiple linear regression in molecular ecology. Mol Ecol Resour. doi: 10.1111/1755-0998.12499

Garrison DL, Buck KR (1986) Organism losses during ice melting: a serious bias in sea ice community studies. Polar Biol 6:237–239

Gems D, Riddle DL (2000) Genetic, behavioral and environmental determinants of male longevity in *Caenorhabditis elegans*. Genetics 154:1597–1610

George JCC, Huntington HP, Brewster K, et al. (2004) Observation on Shorefast Ice Dynamics in Arctic Alaska and the Responses of the Iñupiat Hunting Community. Arctic. doi: 10.14430/arctic514

Gerlach SA, Schrage M (1971) Life cycles in marine meiobenthos. Experiments at various temperatures with *Monhystera disjuncta* and *Theristus pertenuis* (Nematoda). Mar Biol 9:274–280

Golden KM, Ackley SF, Lytle VI (1998) The Percolation Phase Transition in Sea Ice. Science 282:2238–2241. doi: 10.1126/science.282.5397.2238

Gradinger R (1999) Integrated abundance and biomass of sympagic meiofauna in Arctic and Antarctic pack ice. Polar Biol 22:169–177. doi: 10.1007/s003000050407

Gradinger RR, Kaufman MR, Bluhm BA (2009) Pivotal role of sea ice sediments in the seasonal development of near-shore Arctic fast ice biota. Mar Ecol Prog Ser 394:49–63. doi: 10.3354/meps08320

Gradinger RR, Meiners K, Plumley G, et al. (2005) Abundance and composition of the sea-ice meiofauna in off-shore pack ice of the Beaufort Gyre in summer 2002 and 2003. Polar Biol 28:171–181. doi: 10.1007/s00300-004-0674-5

Grainger EH, Mohammed AA, Lovrity JE (1985) The Sea Ice Fauna of Frobisher Bay, Arctic Canada. Arctic 38:23–30

Haarpaintner J, Haugan PM, Gascard JC (2001) Interannual variability of the Storfjorden (Svalbard) ice cover and ice production observed by ERS-2 SAR. Ann Glaciol 33:430–436.

doi: doi:10.3189/172756401781818392

Halinski RS, Feldt LS (1970) The selection of variables in multiple regression analysis. J Educ Meas 7:151–157

Hasegawa M, Kishino H, Yano T (1985) Dating of the human-ape splitting by a molecular clock of mitochondrial DNA. J Mol Evol 22:160–174

Hebert PDN, Cywinska A, Ball SL, deWaard JR (2003) Biological identifications through DNA barcodes. Proceedings Biol Sci 270:313–321. doi: 10.1098/rspb.2002.2218

Holm-Hansen O, Riemann B (1978) Chlorophyll *a* Determination: Improvements in Methodology. Oikos 30:438–447. doi: 10.2307/3543338

Hua E, Mu F, Zhang Z, et al. (2016) Nematode community structure and diversity pattern in sandy beaches of Qingdao, China. J Ocean Univ China 15:33–40

Hutchings P, Kupriyanova E (2018) Cosmopolitan Polychaetes - Fact or Fiction? Personal and Historical Perspectives. Invertebr Syst. doi: 10.1071/IS17035

Hutchings PAT (1998) Biodiversity and functioning of polychaetes in benthic sediments. Biodivers Conserv 1145:

Jacobs LJ, Van De Velde MC, Geraert E, Vranken G (1990) Description of *Diplolaimella dievengatensis* sp. n. (Nematoda: *Monhysteridae*). Nematologica 36:1–21

Jin M, Deal CJ, Wang J, et al. (2006) Controls of the landfast ice–ocean ecosystem offshore Barrow, Alaska. Ann Glaciol 44:63–72

Kauko HM, Olsen LM, Duarte P, et al. (2018) Algal Colonization of Young Arctic Sea Ice in Spring. Front Mar Sci 5:199. doi: 10.3389/fmars.2018.00199

Kedra M, Pabis K, Gromisz S, Wesławski JM (2013) Distribution patterns of polychaete fauna in an Arctic fjord (Hornsund, Spitsbergen). Polar Biol 36:1463–1472. doi: 10.1007/s00300-013-1366-9

Kern JC, Carey AG (1983) The faunal assemblage inhabiting seasonal sea ice in the nearshore Arctic Ocean with emphasis on copepods. Mar Ecol Prog Ser 10:159–167

Kiko R, Kern S, Kramer M, Mütze H (2017) Colonization of newly forming Arctic sea ice by meiofauna: a case study for the future Arctic? Polar Biol 40:1277–1288. doi: 10.1007/s00300-016-2052-5

Kimura M (1980) A simple method for estimating evolutionary rates of base substitutions through comparative studies of nucleotide sequences. J Mol Evol 16:111–120

Kohlbach D, Graeve M, A. Lange B, et al. (2016) The importance of ice algae-produced carbon in the central Arctic Ocean ecosystem: Food web relationships revealed by lipid and stable isotope analyses. Limnol Oceanogr 61. doi: 10.1002/lno.10351

Kohlbach D, Schaafsma FL, Graeve M, et al. (2017) Strong linkage of polar cod (*Boreogadus saida*) to sea ice algae-produced carbon: Evidence from stomach content, fatty acid and stable isotope analyses. Prog Oceanogr 152. doi: 10.1016/j.pocean.2017.02.003

Korbie DJ, Mattick JS (2008) Touchdown PCR for increased specificity and sensitivity in PCR amplification. Nat Protoc 3:13–15. doi: 10.1038/nprot.2008.133

Kramer M (2010) The role of sympagic meiofauna in Arctic and Antarctic sea-ice food webs. The Christian Albrechts Universität zu Kiel

Krembs C, Gradinger R, Spindler M (2000) Implications of brine channel geometry and surface area for the interaction of sympagic organisms in Arctic sea ice. J Exp Mar Bio Ecol 243:55–80. doi: 10.1016/S0022-0981(99)00111-2

Krumpen T, Belter HJ, Boetius A, et al. (2019) Arctic warming interrupts the Transpolar Drift and affects long-range transport of sea ice and ice-rafted matter. Sci Rep 9:5459. doi: 10.1038/s41598-019-41456-y

Kumar S, Stecher G, Tamura K (2016) MEGA7: molecular evolutionary genetics analysis version 7.0 for bigger datasets. Mol Biol Evol 33:1870–1874

Legendre L, Ackley SF, Dieckmann GS, et al. (1992) Ecology of sea ice biota. Polar Biol 12:429–444. doi: 10.1007/BF00243114

Leu E, Graeve M, Wulff A (2016) A (too) bright future? Arctic diatoms under radiation stress. Polar Biol 39:1711–1724. doi: 10.1007/s00300-016-2003-1

Leung TLF, Koprivnikar J (2016) Nematode parasite diversity in birds: the role of host ecology, life history and migration. J Anim Ecol 85:1471–1480

Lønne OJ, Gulliksen B (1989) Size, age and diet of polar cod, *Boreogadus saida* (Lepechin 1773), in ice covered waters. Polar Biol 9:187–191. doi: 10.1007/BF00297174

Lønne OJ, Gulliksen B (1991a) On the distribution of sympagic macro-fauna in the seasonally ice covered Barents Sea. Polar Biol 11:457–469. doi: 10.1007/BF00233081

Lønne OJ, Gulliksen B (1991b) Sympagic macro-fauna from multiyear sea-ice near Svalbard. Polar Biol 11:471–477. doi: 10.1007/BF00233082

Lowther AD, Fisk A, Kovacs KM, Lydersen C (2017) Interdecadal changes in the marine food web along the west Spitsbergen coast detected in the stable isotope composition of ringed seal (*Pusa hispida*) whiskers. Polar Biol 40:2027–2033. doi: 10.1007/s00300-017-2122-3

Madsen H (1936) Investigations on the Shore Fauna of East Greenland with a Survey of the Shores of Other Arctic Regions: Treaarsexpeditionen til Christian den X's Land 1931-34 under Ledelse af Lauge Koch.

Malmgren AJ (1865) Öfversigt af Kongl. Vetenskaps-akademiens forhandlingar. P. A. Norstedt

& Söner

Marquardt M, Kramer M, Carnat G, Werner I (2011) Vertical distribution of sympagic meiofauna in sea ice in the Canadian Beaufort Sea. Polar Biol 34:1887–1900. doi: 10.1007/s00300-011-1078-y

McConnell B, Gradinger R, Iken K, Bluhm BA (2012) Growth rates of arctic juvenile *Scolelepis squamata* (Polychaeta: *Spionidae*) isolated from Chukchi Sea fast ice. Polar Biol 1487–1494. doi: 10.1007/s00300-012-1187-2

Meiners K, Fehling J, Granskog MA, Spindler M (2002) Abundance, biomass and composition of biota in Baltic sea ice and underlying water (March 2000). Polar Biol 25:761–770. doi: 10.1007/s00300-002-0403-x

Michel C, Nielsen TG, Nozais C, Gosselin M (2002) Significance of sedimentation and grazing by ice micro- and meiofauna for carbon cycling in annual sea ice (northern Baffin Bay). Aquat Microb Ecol 30:57–68. doi: 10.3354/ame030057

Müller OF (1776) Zoologiae Danicae prodromus: seu Animalium Daniae et Norvegiae indigenarum; characteres, nomina, et synonyma imprimis popularium. doi: https://doi.org/10.5962/bhl.title.13268

Mundy CJ, Barber DG, Michel C (2005) Variability of snow and ice thermal, physical and optical properties pertinent to sea ice algae biomass during spring. J Mar Syst 58:107–120. doi: https://doi.org/10.1016/j.jmarsys.2005.07.003

Nicholas WL (1975) The biology of free-living nematodes. Clarendon Press.

Norlinder E, Nygren A, Wiklund H, Pleijel F (2012) Phylogeny of scale-worms (Aphroditiformia, Annelida), assessed from 18S rRNA, 28S rRNA, 16S rRNA, mitochondrial cytochrome c oxidase subunit I (COI) and morphology. Mol Phylogenet Evol 65:490–500. doi: 10.1016/j.ympev.2012.07.002

Notz D, Stroeve J (2016) Observed Arctic sea-ice loss directly follows anthropogenic CO2 emission. Science 354:747–750. doi: 10.1126/science.aag2345

Nozais C, Gosselin M, Michel C, Tita G (2001) Abundance, biomass, composition and grazing impact of the sea-ice meiofauna in the North water, Northern Baffin Bay. Mar Ecol Prog Ser 217:235–250. doi: 10.3354/meps217235

Nygren A, Pleijel F (2010) Redescription of *Imajimaea draculai*—a rare syllid polychaete associated with the sea pen *Funiculina quadrangularis*. J Mar Biol Assoc United Kingdom 90:1441–1448

Oliver TH, Heard MS, Isaac NJB, et al. (2015) Biodiversity and Resilience of Ecosystem Functions. Trends Ecol Evol 30:673–684. doi: 10.1016/j.tree.2015.08.009

Olson MA, Zajac RN, Russello MA (2009) Estuarine-scale genetic variation in the polychaete *Hobsonia florida* (*Ampharetidae*; Annelida) in Long Island Sound and relationships to Pleistocene glaciations. Biol Bull 217:86–94

Petersen GH (1962) The distribution of *Balanus balanoides* (L.) and *Littorina saxatilis*, Olivi, var. *groenlandica*, Mencke in Northern West Greenland: with remarks on some causative factors. Danmarks Arktiske Station 33:1-40

Pitusi V (2016) Seasonal development of ice algal biomass and sympagic meiofauna in Van Mijenfjorden, southwest Svalbard. The University Centre in Svalbard

Pitusi V (2019) Seasonal abundance and activity of sympagic meiofauna in Van Mijenfjorden, Svalbard. The University Centre in Svalbard

Porazinska DL, Sung W, Giblin-Davis RM, Thomas WK (2010) Reproducibility of read numbers in high-throughput sequencing analysis of nematode community composition and structure. Mol Ecol Resour 10:666–676

Poulin M, Michel C (2014) Sub-ice colonial *Melosira arctica* in Arctic first-year ice. Diatom Res 29:1–9. doi: 10.1080/0269249X.2013.877085

R Core Team (2019) R: A language and environment for statistical computing. Vienna, Austria http://www.R-project.org/

Ralph MN (2015) Regression and model-building in conservation biology, biogeography and ecology: The distinction between – and reconciliation of – 'predictive' and 'explanatory' models. Biodivers Conserv. doi: DOI: 10.1023/A:1008985925162

Ratnasingham S, Herbert PD (2007) BOLD: The Barcode of Life Data System (www.barcodinglife.org). Mol Ecol Notes. doi: 10.1111/j.1471-8286.2006.01678.x

Rice SA, Karl S, Rice KA (2008) The *Polydora cornuta* complex (Annelida: Polychaeta) contains populations that are reproductively isolated and genetically distinct. Invertebr Biol 127:45–64. doi: 10.1111/j.1744-7410.2007.00104.x

Riemann F, Sime-Ngando T (1997) Note on sea-ice nematodes (*Monhysteroidea*) from Resolute Passage, Canadian high Arctic. Polar Biol 18:70–75

Romeyn K, Bouwman LA (1983) Food selection and consumption by estuarine nematodes. Hydrobiol Bull 17:103–109

Rouse G, Pleijel F (2006) Reproductive Biology and Phylogeny of Annelida

Rousset V, Pleijel F, Rouse GW, et al. (2007) A molecular phylogeny of annelids. Cladistics 23:41–63

Rueden CT, Schindelin J, Hiner MC, et al. (2017) ImageJ2: ImageJ for the next generation of scientific image data. 1–26. doi: 10.1186/s12859-017-1934-z

Sanger F, Nicklen S, Coulson AR (1977) DNA sequencing with chain-terminating inhibitors. Proc Natl Acad Sci 74:5463–5467

Scarpa F, Cossu P, Lai T, et al. (2016) Meiofaunal cryptic species challenge species delimitation: the case of the *Monocelis lineata* (Platyhelminthes: Proseriata) species complex. Contrib to Zool 85:123–145

Schindelin J, Arganda-Carreras I, Frise E, et al. (2012) Fiji: an open-source platform for biological-image analysis. Nat Methods 9:676

Schünemann H (2004) Studies on the Arctic pack-ice habitat and sympagic meiofauna – seasonal and regional variabilities. Der Christian Albrechts Universität zu Kiel

Schünemannn H, Werner I (2005) Seasonal variations in distribution patterns of sympagic meiofauna in Arctic pack ice. Mar Biol 1091–1102. doi: 10.1007/s00227-004-1511-7

Snelgrove PVR (1997) The Importance of Marine Sediment Biodiversity in Ecosystem Processes. Springer 26:578–583

Spearman C (1904) The Proof and Measurement of Association between Two Things. Am J Psychol 15:72–101. doi: 10.2307/1412159

Spindler M, Dieckmann GS (1986) Distribution and abundance of the planktic foraminifer *Neogloboquadrina pachyderma* in sea ice of the Weddell Sea (Antarctica). Polar Biol 5:185–191. doi: 10.1007/BF00441699

Stroeve J, Notz D (2018) Changing state of Arctic sea ice across all seasons. Environ Res Lett

Szymelfenig M, Kwasniewski S, Weslawski J (1997) Intertidal zone of Svalbard. Polar Biol 18:45–52. doi: 10.1007/s003000050157

Tchesunov A, Portnova D (2005) Free-living nematodes in seasonal coastal ice of the White Sea. Description of *Hieminema obliquorum* gen. et sp. n. (Nematoda, *Monhysteroidea*). Zool Zhurnal

Tchesunov A V, Portnova DA (2015) Description of two free-living nematode species of *Halomonhystera disjuncta* complex (Nematoda: Monhysterida) from two peculiar habitats in the sea. Helgol Mar Res 57–85. doi: 10.1007/s10152-014-0416-1

Tchesunov A V, Portnova DA (2003) Nematode population in the coastal seasonal ice of the White Sea. Russian Society of Nematologists, Vladivostok

Tchesunov A V, Riemann F (1995) Arctic Sea Ice Nematodes (*Monhysteroidea*) with Descriptions of *Cryonema crassum* gen. n., sp. n. and *C. tenue* sp. n. Nematologica 41:35–50

Telenius A, Shah M (2016) Invertebrates Collection of the Swedish Museum of Natural History. GBIF-Sweden. Occurrence dataset. GBIF.org. Accessed 27 May 2019

Thomas DN, Dieckmann GS (2009) Sea Ice, 2nd edn. Wiley

Thomsen MS, Godbold JA, Garcia C, et al. (2019) Compensatory responses can alter the form of the biodiversity – function relation curve. Proc R Soc B

Timco GW, Frederking RMW (1996) A review of sea ice density. Cold Reg Sci Technol 24:1–6. doi: https://doi.org/10.1016/0165-232X(95)00007-X

Truett GE, Heeger P, Mynatt RL, et al. (2000) Preparation of PCR-quality mouse genomic DNA with hot sodium hydroxide and tris (HotSHOT). Biotechniques 29:52,54. doi: 10.2144/00291bm09

UNIS Board (2017) UNIS Annual Report 2017

Van Campenhout J, Derycke S, Tchesunov A, et al. (2014) The *Halomonhystera disjuncta* population is homogeneous across the Håkon Mosby mud volcano (Barents Sea) but is genetically differentiated from its shallow-water relatives. J Zool Syst Evol Res 52:203–216. doi: 10.1111/jzs.12054

van Leeuwe MA, Tedesco L, Arrigo KR, et al. (2018) Microalgal community structure and primary production in Arctic and Antarctic sea ice: a synthesis. Elem Sci Anth 6. doi: 10.1525/elementa.267

Vanaverbeke J, Arbizu PM, Dahms HU, Schminke HK (1997) The metazoan meiobenthos along a depth gradient in the Arctic Laptev Sea with special attention to nematode communities. Polar Biol 18:391–401. doi: 10.1007/s003000050205

Wassmann P, Duarte CM, Agustí S, Sejr MK (2011) Footprints of climate change in the Arctic marine ecosystem. Glob Chang Biol 1235–1249. doi: 10.1111/j.1365-2486.2010.02311.x

Werner I (2005) Living conditions, abundance and biomass of under-ice fauna in the Storfjord area (western Barents Sea, Arctic) in late winter (March 2003). Polar Biol 28:311–318. doi: 10.1007/s00300-004-0678-1

Wirén, A (1883) Chaetopoder från Sibiriska Ishafved och Berings Haf Insamlade under Vega-Expeditionen 1878-1879. Vega-Expeditionens Vetenskapliga Iakttagelser bearbetade af deltagare i resan och andra forskare. 2:383-428, plates 27-32.

Zhang J, Spitz YH, Steele M, et al. (2010) Modeling the impact of declining sea ice on the Arctic marine planktonic ecosystem. J Geophys Res Ocean 115:1–24. doi: 10.1029/2009JC005387

Supporting information

Appendix 1. Station coordinates
Appendix 2. Site description of Wahlenbergfjorden and Palanderbukta with notes on methodology
Appendix 3. Site description of Van Mijenfjorden
Appendix 4. Sea ice charts
Appendix 5. Field site photographs
Appendix 6. Model selection, construction and testing
Appendix 7. Primer overview
Appendix 8. Accession numbers
Appendix 9. Sympagic algae in Agardhbukta
Appendix 10. Chain of *Melosira arctica*
Appendix 11. Sympagic and pelagic meiofauna
Appendix 12. Reference names
Appendix 13. Registrations of selected polychaetes and nematodes in the Arctic
Appendix 14. Conceptual figure on trophic dynamics under different snow depths

Appendix 1. Station coordinates

Table 1. Coordinates and depth of stations in Inglefieldbukta (IB) and Agardhbukta (AGA) along with depth transect stations in Inglefieldbukta.

Station	Date	Station depth (m)	Pos °N	Pos °E
IB1	22.03/26.04.18	4	77°53.255	18°16.227
IB2	23.03.18	32	77°53.453	18°14.302
IB3	27.04.18	32	77°53.282	18°13.768
AGA	15.04.18	42	78°00.580	18°34.426
Depth 1	23.03.18	24	77°53.453	18°14.302
Depth 2	23.03.18	28	77°53.660	18°15.566
Depth 3	23.03.18	17	77°53.767	18°16.409
Depth 4	23.03.18	13	77°53.844	18°17.101
Depth 5	23.03.18	9	77°53.909	18°17.815
Depth 6	23.03.18	10	77°53.988	18°18.553

Appendix 2. Site description of Wahlenbergfjorden and Palanderbukta with notes on methodology

Wahlenbergfjorden is a 50 km long east-west directed fjord terminating to the Hinlopen Strait in northern Svalbard at 79°41 N 19°21 E. At the southern shore, 10 km from the fjord mouth, the 35 km long Palanderbukta branches of in a northwest-southeast direction (Fig. 1). Depth maxima are 290 m and 120 m for Wahlenbergfjorden and Palanderbukta, respectively, with exposed bedrock as the main bottom substrate (Flink et al. 2014).

Figure 1. Wahlenbergfjorden and Palanderbukta, northern Svalbard, with depth (HTR) and six sampling stations along the sea ice edge 18th of June 2018.

Wahlenbergfjorden

Sea ice pieces (volume not quantified) were collected from R/V Helmer Hansen, 5th of May 2018 at 79°42.157' N, 20°21.287' E. Filtered sea water (0.7 µm) was added and samples were stored cold and dark until further analysis as described for sea ice cores in the main paper.

Palanderbukta

Three sea ice samples (~ 0.1 m^3) were collected along the sea ice edge in Palanderbukta, 18th of June 2018. By the same locations, a 20 µm plankton net was hauled to 18 m once 10 meters perpendicular from the ice edge (Fig. 1). Depths measured using the echo sounder from M/S Spitsbergen 600 m west of the sample site represent the accessible bathymetric data (Table 1).

Table 1. Sample stations and depth station (HTR) in Palanderbukta, Svalbard.

Station	Date	n	Time	Station depth (m)	Pos °N	Pos °E
water1	18.06.18	1	14:00 – 15:00	–	79°34.427'	20°40.049'
ice1	18.06.18	1	14:00 – 15:00	–	79°34.423'	20°40.133'
water2	18.06.18	1	14:00 – 15:00	–	79°34.525'	20°40.170'
ice2	18.06.18	1	14:00 – 15:00	–	79°34.516'	20°40.250'
water3	18.06.18	1	14:00 – 15:00	–	79°34.705'	20°40.572'
ice3	18.06.18	1	14:00 – 15:00	–	79°34.693'	20°40.703'
HTR	18.06.18	–	17:40	69	79°34.474'	20°37.991'

Appendix 3. Site description of Van Mijenfjorden

Van Mijenfjorden is situated in western Svalbard at 78 °N 16 °E partially separated from the Atlantic influenced West Spitsbergen Current by Akseløya (Fig. 2). The fjord is 60 km long and on average 10 km wide with numerous glaciers and glacial rivers characterizing the coast. The bathymetry is characterized by two basins; an inner shallower of up to 74 m and an outer with depths up to 115 m. Moreover, the currently inactive coalmine Svea is located in the northeastern part. Compared to Agardhbukta and especially Inglefieldbukta, Van Mijenfjorden is subject to considerable motorized traffic, i.e. snow mobiles on sea ice and shores during spring, aviation throughout the year and industrial marine vessels most frequently during open-water periods.

Figure 1. Van Mijenfjorden in western Svalbard with reference sampling stations VMF, VMF30 and VMF1 from Pitusi (2019)

Appendix 4. Sea ice charts

Figure 1. Sea ice charts (02.01.18 – 15.06.18) from Storfjorden area displaying southeastern ice edge dynamics estimated from satellite imagery (Norwegian Meteorological Institute). Bold dates represent dates of sampling.

Appendix 5. Field site photographs

Aerial photography was applied when the snow and ice topography surrounding the station was not homogenous. In Agardhbukta, 15.04.18, a wave-like structure characterized the sea ice with consequences for the distribution of snow cover (Fig. 1). In Inglefieldbukta at IB3, 27.04.18, glacial ice was incorporated into the sea ice with implications for the topography and, most likely, salinity (Fig. 2).

Figure 1. Station in Agardhbukta, 15.04.18, with visible heterogeneous distribution of snow.

Figure 2. Station (IB3) in Inglefieldbukta, 27.04.18, with visible glacial ice pieces in the nearby surroundings.

Appendix 6. Model selection, construction and testing

A model was constructed for the following hypotheses:
H_0: Sympagic polychaete juvenile length does not differ from March to May in neither east Svalbard (Inglefieldbukta/Agardhbukta) or west Svalbard (Van Mijenfjorden)

Variables
Dependent: Continuous (sympagic polychaete juvenile length)
Independent: Continuous (day number) and categorical (east Svalbard or west Svalbard)
Model: Multiple linear regression (analysis of covariance, ANCOVA, in R; Eq. 1)

$$Length_{poly} = -126.7 + 5.6 \times day\ number + 96.1 \times site \qquad Eq.\ 1$$

Assumptions
- Similar environmental conditions in the sample years 2017 and 2018

Pitfalls
Multicollinearity
- Tested against using the backward elimination method (Halinski and Feldt 1970) including the interaction term *site:day number*

Autocorrelation
- Both time (day number) and place (east or west) is included as independent variables in this model and considering temporal and spatial autocorrelation is consequently not relevant

Excluding important predictor variables
- Multiple predictor variables should be included in future attempts to explain the processes underlying polychaete growth, *inter alia* nutrient availability, temperature, salinity, competition for nutrients and space

Power and sample size
- The power of this model is limited by low temporal resolution and sample size. It should therefore serve as a reference model until further data on the included variables are accessible

Model testing
Testing of homoscedasticity, multicollinearity and normal distribution (Quantile-Quantile plots) was done in in R (R Core Team 2019).

Appendix 7. Primer overview

Table 1. Primers applied in molecular analyses of polychaetes (COI) and nematodes (18S rRNA) in this study. Base pairs = number of base pairs expected, Poly = polychaete, Nema = nematode.

Primer ID	Sequence	Base pairs	Target	Reference
polyLCO (F)	GAYTATWTTCAACAAATCATAAAGATATTGG	710	Poly COI	Carr et al. (2011)
polyHCO (R)	TAMACTTCWGGGTGACCAAARAATCA			
miCOlint F	GGWACWGGWTGAACWGTWTAYCCYCC	313	COI	Leray et al. (2013)
jgHCO2190	TAIACYTCIGGRTGICCRAARAAYCA			Geller et al. (2013)
MN18F	CGCGAATRGCTCATTACAACAGC	925	Nema 18S	Bhadury et al. (2006)
Nem_18S_R	CGCGAATRGCTCATTACAACAGC			

Appendix 8. Accession numbers

Sequences on *Halomonhystera disjuncta* (previously *Geomonhystera disjuncta*; GD; Bastian 1865) are available in Van Campenhout et al. (2014; *supplementary material*).

Table 1. Accession numbers for voucher polychaete species from NCBI's GenBank included in phylogenetic analyses in this study.

Accession no.	Description	Origin	Reference	Gene
HM417792.1	*Bylgides* BOLD	White Sea	Carr, *unpubl.*	COI
HQ024272.1	*Bylgides groenlandicus*	Canadian Arctic	Carr et al. 2011	COI
HM473329.1	*Bylgides macrolepidus*	British Columbia	Carr et al. 2011	COI
HQ024273.1	*Bylgides promamme*	Canadian Arctic	Carr et al. 2011	COI
HQ024300.1	*Eunoe nodosa* CMC01	Canadian Arctic	Carr et al. 2011	COI
HQ023873.1	*Eunoe nodosa CMC02*	Canadian Arctic	Carr et al. 2011	COI
HQ023872.1	*Eunoe nodosa CMC02*	Canadian Arctic	Carr et al. 2011	COI
HQ024302.1	*Eunoe nodosa* CMC02	Canadian Arctic	Carr et al. 2011	COI
HQ024301.1	*Eunoe nodosa* CMC02	Canadian Arctic	Carr et al. 2011	COI
HM473743.1	*Eunoe oerstedi* CMC01	Chukchi Sea	Carr et al. 2011	COI
HM473742.1	*Eunoe oerstedi* CMC01	Chukchi Sea	Carr et al. 2011	COI
HM473741.1	*Eunoe oerstedi* CMC01	Chukchi Sea	Carr et al. 2011	COI
HM473740.1	*Eunoe oerstedi* CMC01	Chukchi Sea	Carr et al. 2011	COI
HQ024020.1	*Eunoe oerstedi* CMC02	Canadian Arctic	Carr et al. 2011	COI
MF121623.1	*Eunoe* sp. 11BIOAK	Cook Inlet	Carr, *unpubl.*	COI
MF121462.1	*Eunoe* sp. 11BIOAK	Cook Inlet	Carr, *unpubl.*	COI
MF121029.1	*Eunoe* sp. 11BIOAK	Cook Inlet	Carr, *unpubl.*	COI
GU672348.1	*Eunoe* sp. BOLD	Canadian Arctic	Carr et al. 2011	COI
GU672336.1	*Eunoe* sp. BOLD	Canadian Arctic	Carr et al. 2011	COI
MH242753.1	*Eunoe* sp. FHL1	Washington	Leray & Paulay, *unpubl.*	COI
HM473744.1	*Eunoe spinicirris*	Chukchi Sea	Carr et al. 2011	COI
JN852936.1	*Melaenis loveni*	Svalbard	Norlinder et al. (2012)	COI

Table 1, continued. Accession numbers for voucher polychaete species from NCBI's GenBank included in phylogenetic analyses in this study.

Accession no.	Description	Origin	Reference	Gene
HM473680.1	*Scolelepis squamata*	Vancouver Island	Carr et al. 2011	COI
HM473679.1	*Scolelepis squamata*	Vancouver Island	Carr et al. 2011	COI
HQ932541.1	*Scolelepis squamata*	Vancouver Island	Jeffery et al., *unpubl.*	COI
MF120984.1	*Scolelepis squamata*	Gulf of Alaska	Carr et al., *unpubl.*	COI
MF121430.1	*Scolelepis squamata*	Gulf of Alaska	Carr et al., *unpubl.*	COI
MF121675.1	*Scolelepis squamata*	Gulf of Alaska	Carr et al., *unpubl.*	COI
GU672125.1	*Spio* sp. CMC01	Canadian Arctic	Carr et al. 2011	COI
HQ024469.1	*Spio* sp. CMC01	Canadian Arctic	Carr et al. 2011	COI
HQ024470.1	*Spio* sp. CMC01	Canadian Arctic	Carr et al. 2011	COI
HQ024471.1	*Spio* sp. CMC01	Canadian Arctic	Carr et al. 2011	COI
HQ024472.1	*Spio* sp. CMC01	Canadian Arctic	Carr et al. 2011	COI
HQ024474.1	*Spio* sp. CMC01	Canadian Arctic	Carr et al. 2011	COI
GU672142.1	*Spio* sp. CMC02	Canadian Arctic	Carr et al. 2011	COI
GU672196.1	*Spio* sp. CMC02	Canadian Arctic	Carr et al. 2011	COI
GU672212.1	*Spio* sp. CMC02	Canadian Arctic	Carr et al. 2011	COI
GU672214.1	*Spio* sp. CMC02	Canadian Arctic	Carr et al. 2011	COI
GU672316.1	*Spio* sp. CMC02	Canadian Arctic	Carr et al. 2011	COI
GU672349.1	*Spio* sp. CMC02	Canadian Arctic	Carr et al. 2011	COI
GU672398.1	*Spio* sp. CMC02	Canadian Arctic	Carr et al. 2011	COI
HQ023786.1	*Spio* sp. CMC02	Canadian Arctic	Carr et al. 2011	COI
HQ561107.1	*Spio* sp. CMC02	Canadian Arctic	Carr et al. 2011	COI
GU672334.1	*Spio* sp. CMC03	Canadian Arctic	Carr et al. 2011	COI
GU672335.1	*Spio* sp. CMC03	Canadian Arctic	Carr et al. 2011	COI
HQ023787.1	*Spio* sp. CMC03	Canadian Arctic	Carr et al. 2011	COI
HQ023788.1	*Spio* sp. CMC03	Canadian Arctic	Carr et al. 2011	COI
HQ023789.1	*Spio* sp. CMC03	Canadian Arctic	Carr et al. 2011	COI
HQ023790.1	*Spio* sp. CMC03	Canadian Arctic	Carr et al. 2011	COI
HQ023791.1	*Spio* sp. CMC03	Canadian Arctic	Carr et al. 2011	COI
HQ023792.1	*Spio* sp. CMC03	Canadian Arctic	Carr et al. 2011	COI
HQ024476.1	*Spio* sp. CMC03	Canadian Arctic	Carr et al. 2011	COI
HQ024475.1	*Spio* sp. CMC03	Canadian Arctic	Carr et al. 2011	COI
MG670060.1	*Theristus acer*	Netherlands	Macheriotou et al., *unpubl.*	18S
MG670062.1	*Theristus ensifer*	Netherlands	Macheriotou et al., *unpubl.*	18S
MG670070.1	*Theristus* sp.	Netherlands	Macheriotou et al., *unpubl.*	18S

Appendix 9. Sympagic algae in Agardhbukta

Table 1. Sympagic algae registered in Agardhbukta (AGA) 15th of April 2018. Most dominant species are bold.

Taxa	AGA April
Armoured dinoflagellate	0
Ceratium arcticum	0
Cf. Gyrosigma fascida	0
Chaetoceros sp.	1
Cylidrotheca closterium	1
Dictyocha speculum	0
Dinophysis rotundata	1
Entomoneis sp.	1
Fragilaropsis cylindrus	0
Gymnodiniacae sp.	1
***Haslea* sp.**	1
Navicula levissima	1
Navicula septentrionalis	1
Nitzschia frigida	1
Nitzschia promare	1
Pauliella taentiata	1
Pleurosigma sp.	0
Protoperidinium breve	0
Pterosperma vanhoeffenii	0
Thalassiosira antarctica/gravia	1

Appendix 10. Chain of *Melosira arctica*

At IB1 in Inglefieldbukta, 26.04.18, long chains of *Melosira arctica* were observed at the lower 1 cm section sea ice (Fig. 1). The observation was confirmed by Jósef Wiktor (*personal communication*, May 2018).

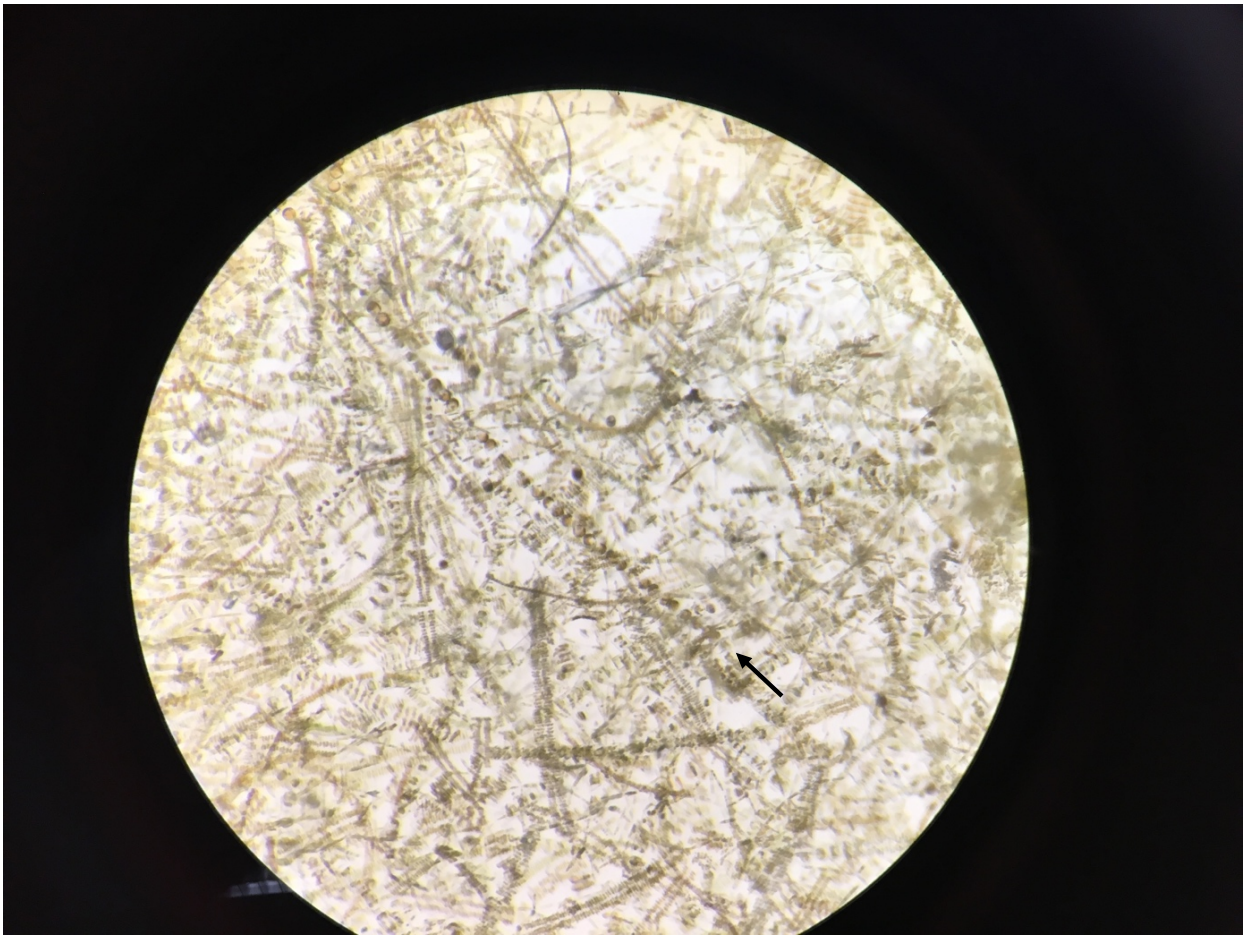

Figure 1. Chain of *Melosira arctica* (black arrow) from sea ice in Inglefieldbukta, Svalbard, 26.04.18.

Appendix 11. Sympagic and pelagic meiofauna

Table 1. Sympagic and pelagic meiofauna (ind. $m^{-2} \pm$ SD) in Inglefieldbukta (IB) and Agardhbukta (AGA) in spring 2018. Degr. poly. juv. = degraded polychaete juvenile.

Taxa	IB1 March	IB2 March	AGA April	IB1 April	IB3 April
Sympagic					
Polychaete juv.	208.7 ± 150	300.4 ± 139	4321.7 ± 1878	4596.7 ± 2583	0.0
Nematoda	219.7 ± 138	1913.4 ± 936	0.0	407.6 ± 236	2051.3 ± 1382
Trochophora	0.0	0.0	1271.0 ± 298	0.0	0.0
Rotifera	0.0	0.0	347.3 ± 128	395.4 ± 153	0.0
Ciliata			351.9 ± 104	1723.5 ± 418	401.9 ± 166
Eggs	0.0	263.0 ± 125	7998.4 ± 2742	1903.1 ± 1252	0.0
Unidentified	0.0	59.3 ± 52	0.0	5189.3 ± 3368	0.0
Pelagic					
Polychate juv.		2.0			0.0
Nematoda		42.0			0.0
Copepoda		38.0			75.3 ± 28.0
Cop. nauplii		212.0			98.7 ± 95.3
Ophiopluteus		0.0			3.3 ± 4.2
Sarsia		0.0			0.7 ± 1.2
Other hydrozoa		0.0			0.7 ± 1.5
Bivalvia veliger		4.0			1.3 ± 2.3
Chaetognatha		0.0			2.0 ± 3.5
Eggs		2.0			78.7 ± 43.1
Unidentified		0.0			4.0 ± 4.0
Degr. poly. juv.		0.0			16.7 ± 28.9

Appendix 12. Reference names

Table 1. Reference names for polychaetes displayed in phylogenetic trees.
IB = Inglefieldbukta, VMF = Van Mijenfjorden.

Ref. Name	Phylum	Ref #	Station	Date	Reference
IB1A1	*Polychaeta*	59FF51	IB1	26.04.18	Andreasen et al. 2019, *unpubl.*
IB1A2	*Polychaeta*	59FF67	IB1	26.04.18	Andreasen et al. 2019, *unpubl.*
IB1A3	*Polychaeta*	59FF61	IB1	26.04.18	Andreasen et al. 2019, *unpubl.*
IB1A4	*Polychaeta*	59FF53	IB1	26.04.18	Andreasen et al. 2019, *unpubl.*
IB1A5	*Polychaeta*	59FF59	IB1	26.04.18	Andreasen et al. 2019, *unpubl.*
IB1A6	*Polychaeta*	59FF55	IB1	26.04.18	Andreasen et al. 2019, *unpubl.*
IB1A7	*Polychaeta*	59FF57	IB1	26.04.18	Andreasen et al. 2019, *unpubl.*
IB1A8	*Polychaeta*	59FF93	IB1	26.04.18	Andreasen et al. 2019, *unpubl.*
IB1A9	*Polychaeta*	59FF73	IB1	26.04.18	Andreasen et al. 2019, *unpubl.*
IB1A10	*Polychaeta*	59FF69	IB1	26.04.18	Andreasen et al. 2019, *unpubl.*
VMF1	*Polychaeta*	59FG47	VMF30	28.04.18	Pitusi et al. 2018, *unpubl.*
VMF2	*Polychaeta*	59FG45	VMF30	28.04.18	Pitusi et al. 2018, *unpubl.*
VMF3	*Polychaeta*	59FG43	VMF30	28.04.18	Pitusi et al. 2018, *unpubl.*

Table 2. Reference names for nematodes displayed in phylogenetic trees.
IB = Inglefieldbukta, VMF = Van Mijenfjorden.

Ref. name	Phylum	Ref #	Station	Date	Reference
PAL1	*Nematoda*	59FF47	PAL	18.06.18	Andreasen et al. 2019, *unpubl.*
PAL2	*Nematoda*	59FF43	PAL	18.06.18	Andreasen et al. 2019, *unpubl.*
IB1M1	*Nematoda*	59FG03	IB1	22.03.18	Andreasen et al. 2019, *unpubl.*
IB2M1	*Nematoda*	59FG19	IB2	23.03.18	Andreasen et al. 2019, *unpubl.*
IB2M2	*Nematoda*	59FG17	IB2	23.03.18	Andreasen et al. 2019, *unpubl.*
IB2M3	*Nematoda*	59FG15	IB2	23.03.18	Andreasen et al. 2019, *unpubl.*
IB2M4	*Nematoda*	59FG13	IB2	23.03.18	Andreasen et al. 2019, *unpubl.*
IB2M5	*Nematoda*	59FG12	IB2	23.03.18	Andreasen et al. 2019, *unpubl.*
IB2M6	*Nematoda*	59FG09	IB2	23.03.18	Andreasen et al. 2019, *unpubl.*
IB2M7	*Nematoda*	59FG07	IB2	23.03.18	Andreasen et al. 2019, *unpubl.*
IB2M8	*Nematoda*	59FG05	IB2	23.03.18	Andreasen et al. 2019, *unpubl.*
VMF4	*Nematoda*	06BI80	VMF	23.04.17	Pitusi et al. 2017, *unpubl.*
VMF5	*Nematoda*	06BI58	VMF	08.03.17	Pitusi et al. 2017, *unpubl.*
VMF6	*Nematoda*	06BI83	VMF1	07.04.17	Pitusi et al. 2017, *unpubl.*
VMF7	*Nematoda*	06BI86	VMF	08.03.17	Pitusi et al. 2017, *unpubl.*
VMF8	*Nematoda*	06BI90	VMF	08.03.17	Pitusi et al. 2017, *unpubl.*
VMF9	*Nematoda*	06BI92	VMF	08.03.17	Pitusi et al. 2017, *unpubl.*
VMF10	*Nematoda*	06BJ07	VMF	23.04.17	Pitusi et al. 2017, *unpubl.*
VMF11	*Nematoda*	06BJ32	VMF	08.03.17	Pitusi et al. 2017, *unpubl.*
VMF12	*Nematoda*	06BJ34	VMF	08.03.17	Pitusi et al. 2017, *unpubl.*
VMF13	*Nematoda*	06BJ36	VMF	08.03.17	Pitusi et al. 2017, *unpubl.*
VMF14	*Nematoda*	06BJ38	VMF	08.03.17	Pitusi et al. 2017, *unpubl.*
VMF15	*Nematoda*	06CF07	VMF	08.03.17	Pitusi et al. 2017, *unpubl.*
VMF16	*Nematoda*	06CF09	VMF1	07.04.17	Pitusi et al. 2017, *unpubl.*
VMF17	*Nematoda*	06CF11	VMF	08.03.17	Pitusi et al. 2017, *unpubl.*
VMF18	*Nematoda*	06CF13	VMF	08.03.17	Pitusi et al. 2017, *unpubl.*
VMF19	*Nematoda*	06CF17	VMF	08.03.17	Pitusi et al. 2017, *unpubl.*

Table 2, continued. Reference names for nematodes displayed in phylogenetic trees.
IB = Inglefieldbukta, VMF = Van Mijenfjorden.

VMF20	*Nematoda*	06CF19	VMF1	07.04.17	Pitusi et al. 2017, *unpubl.*
VMF21	*Nematoda*	06CF21	VMF	08.03.17	Pitusi et al. 2017, *unpubl.*
VMF22	*Nematoda*	06CF23	VMF	08.03.17	Pitusi et al. 2017, *unpubl.*
VMF23	*Nematoda*	06CF25	VMF	08.03.17	Pitusi et al. 2017, *unpubl.*
VMF24	*Nematoda*	06CF27	VMF	08.03.17	Pitusi et al. 2017, *unpubl.*
VMF25	*Nematoda*	06CF29	VMF	08.03.17	Pitusi et al. 2017, *unpubl.*
VMF26	*Nematoda*	06CF30	VMF	08.03.17	Pitusi et al. 2017, *unpubl.*
VMF27	*Nematoda*	06CF32	VMF1	07.04.17	Pitusi et al. 2017, *unpubl.*
VMF28	*Nematoda*	06CF35	VMF1	07.04.17	Pitusi et al. 2017, *unpubl.*
VMF29	*Nematoda*	06CF37	VMF1	07.04.17	Pitusi et al. 2017, *unpubl.*
VMF30	*Nematoda*	06CF41	VMF1	07.04.17	Pitusi et al. 2017, *unpubl.*
VMF31	*Nematoda*	06CF43	VMF	06.04.17	Pitusi et al. 2017, *unpubl.*
VMF32	*Nematoda*	06CF47	VMF	06.04.17	Pitusi et al. 2017, *unpubl.*
VMF33	*Nematoda*	06CF52	VMF	06.04.17	Pitusi et al. 2017, *unpubl.*
VMF34	*Nematoda*	06CF55	VMF	06.04.17	Pitusi et al. 2017, *unpubl.*
VMF35	*Nematoda*	06CF61	VMF	06.04.17	Pitusi et al. 2017, *unpubl.*
VMF36	*Nematoda*	06CF67	VMF	23.04.17	Pitusi et al. 2017, *unpubl.*
VMF37	*Nematoda*	06CF74	VMF	06.04.17	Pitusi et al. 2017, *unpubl.*
VMF38	*Nematoda*	06CF80	VMF	23.04.17	Pitusi et al. 2017, *unpubl.*
VMF39	*Nematoda*	06CF83	VMF	23.04.17	Pitusi et al. 2017, *unpubl.*
VMF40	*Nematoda*	91AD54	VMF	–	Pitusi et al. 2017, *unpubl.*
VMF41	*Nematoda*	91AD56	VMF	–	Pitusi et al. 2017, *unpubl.*
VMF42	*Nematoda*	91AD62	VMF	–	Pitusi et al. 2017, *unpubl.*
VMF43	*Nematoda*	06CF75	VMF	06.04.17	Pitusi et al. 2017, *unpubl.*
VMF44	*Nematoda*	06CF58	VMF	06.04.17	Pitusi et al. 2017, *unpubl.*
WB1	*Nematoda*	59FG01	VMF	05.05.18	Andreasen et al. 2019, *unpubl.*
WB2	*Nematoda*	59FG00	VMF	05.05.18	Andreasen et al. 2019, *unpubl.*
VMF45	*Nematoda*	91AD59	VMF	–	Pitusi et al. 2017, *unpubl.*

Appendix 13. Conceptual figure on trophic dynamics under different snow depths

In the discussion section, I evaluated the potential influence of decreased irradiance, as a result of the greater snow depth, on the sympagic community at IB3 in April compared to IB1 and AGA in April. Figure 1 illustrates the concepts behind the reasoning in this paper and builds upon results by Kramer (2010).

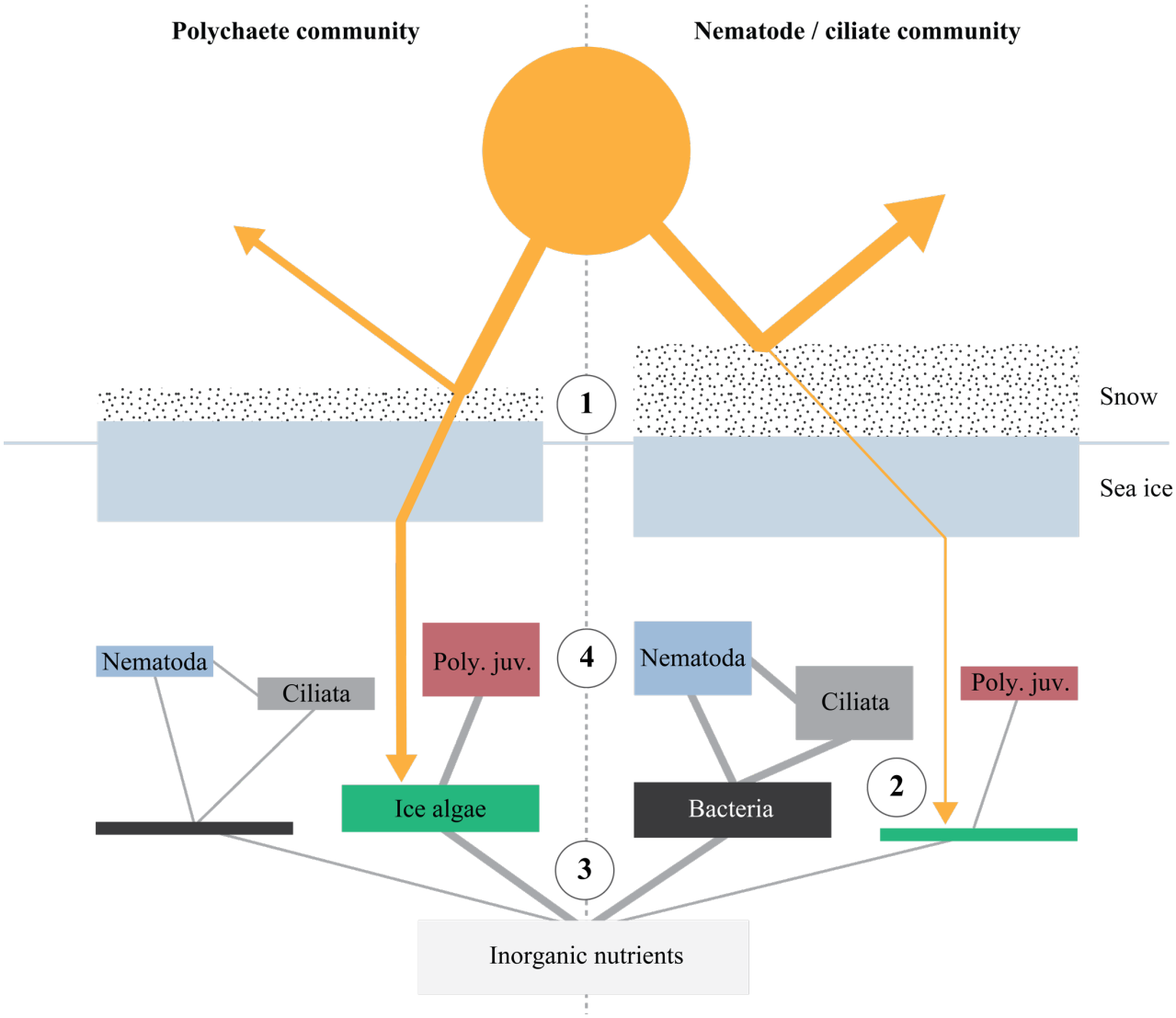

Figure 1. Conceptual illustration of potential trophic responses to different snow depths. 1: snow depth determines the level of irradiance available to sympagic algae, 2: a too thick snow layer inhibits photosynthesis and hampers sympagic algae production, 3: the proportion of inorganic nutrients being assimilated by sympagic algae or bacteria will depend on the light saturation of sympagic algae, 4: the community will be dominated by either polychates (Poly. juv.) or nematodes and ciliates. The illustration assumes that polychaetes largely graze on sympagic algae, while nematodes and ciliates feed on bacteria (Kramer 2010). In addition, the illustration assumes an intermediate snow depth in the polychaete-dominated community, yielding an optimal light climate for sympagic algae (Mundy et al. 2005). The concept will hence not apply in radiation-stressed communities (Leu et al. 2016).

Appendix 14. Registrations of selected polychaetes and nematodes in the Arctic

Figure 1. Published benthic registrations of *Melaenis loveni* at depths from 5-162 m.

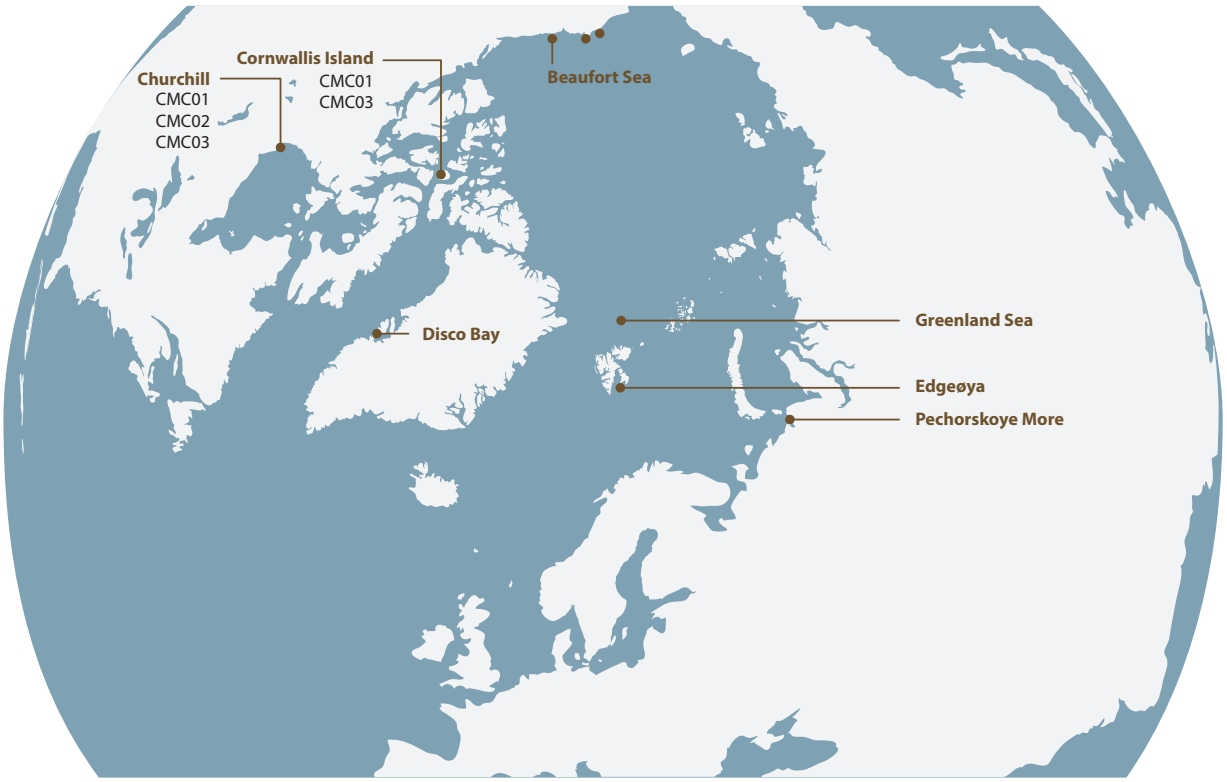

Figure 2. Published benthic registrations of *Spio* spp. at depths from 2-150 m above the Arctic Circle. CMC01-03 represent registrations by Carr et al. (2011) included herein.

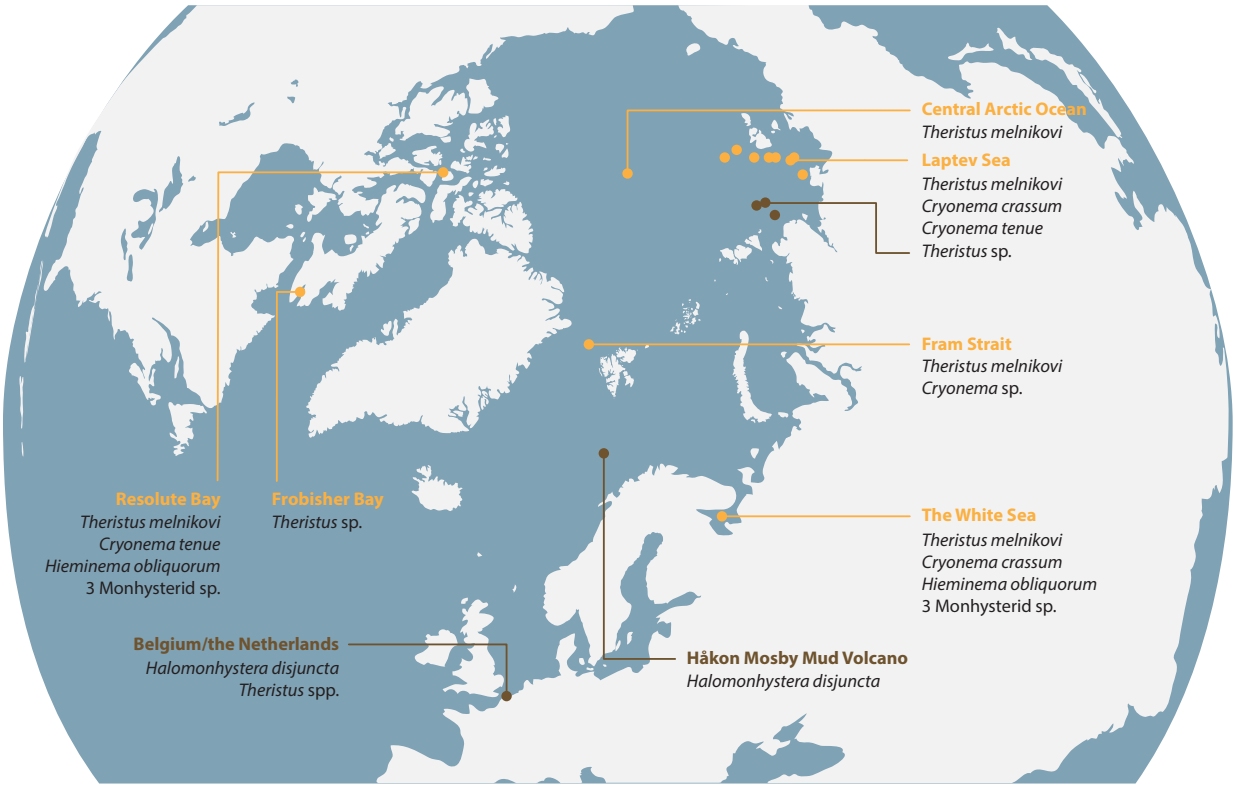

Figure 3. Published registrations of *Theristus melnikovi, Theristus* sp., *Cryonema crassum, C. tenue, Cryonema* sp., *Hieminema obliquorum* and three species belonging to *Monhysteridae* in sea ice (orange) and benthos (brown).

Table 1. Collectors of species illustrated in Figure 1, 2 and 3 above. Specimens included in Appendix 8: Accession numbers are not included. References comprise data on the listed collectors (Blum and Fong 2016; Telenius and Shah 2016).

Station	Species	Collector	Year collected	Database / reference
Kongsøya	*Melaenis loveni*	Kolthoff and Ohlin	1898	Telenius and Shah (2016)
Storfjorden	*Melaenis loveni*	Malmgren	1864	Telenius and Shah (2016)
Sørkapp	*Melaenis loveni*	Malmgren	1866	Telenius and Shah (2016)
Van Mijenfjorden	*Melaenis loveni*	Wirén	1883	Telenius and Shah (2016)
Kongsfjorden	*Melaenis loveni*	Goës	1861	Telenius and Shah (2016)
Widjefjorden	*Melaenis loveni*	Pleijel	2003	Telenius and Shah (2016)
Beaufort Sea	*Melaenis loveni*	Dickinson; Broad, Dunton	1976; 77; 78	Telenius and Shah (2016)
Chuckchi Sea	*Melaenis loveni*	Stuxberg, Nordquist and Stuxberg	1878; 79	Telenius and Shah (2016)
Baffin Bay	*Melaenis loveni*	Nilson	1894	Telenius and Shah (2016)
Hurry Fjord	*Melaenis loveni*	Arwidsson	1899	Telenius and Shah (2016)
Coronation Gulf	*Melaenis loveni*	Miller	2012	Telenius and Shah (2016)
Edgeøya	*Spio filicornis*	Malmgren	1864	Telenius and Shah (2016)
North of Svalbard	*Spio filicornis*	Kolthoff and Ohlin	1878	Telenius and Shah (2016)
Pechorskoye More	*Spio filicornis*	Stuxberg	1878	Telenius and Shah (2016)
Beaufort Sea	*Spio filicornis*	Schneider	1977	Blum and Fong (2016)
Disco Bay	*Spio filicornis*	Disco Bay	1870	Blum and Fong (2016)
Central Arctic Ocean	*Theristus melnikovi*			Tchesunov and Riemann (1995)
Laptev Sea	*Theristus melnikovi*			Tchesunov and Riemann (1995)
	Cryonema crassum			Tchesunov and Riemann (1995)
	Cryonema tenue			Tchesunov and Riemann (1995)
	Theristus sp.			Vanaverbeke (1993)
Fram Strait	*Theristus melnikovi*			Tchesunov and Riemann (1995)
	Cryonema sp.			Tchesunov and Riemann (1995)
The White Sea	*Theristus melnikovi*			Tchesunov and Portnova (2005)
	Cryonema crassum			Tchesunov and Portnova (2005)
	Hieminema obliquorum			Tchesunov and Portnova (2005)
	3 *Monhysteridae* sp.			Tchesunov and Portnova (2005)
Resolute Bay	*Theristus melnikovi*			Riemann and Ngando (1997)
	Cryonema tenue			Riemann and Ngando (1997)
	Hieminema obliquorum			Riemann and Ngando (1997)
	3 Monhysteridae sp.			Riemann and Ngando (1997)
Frobisher Bay	*Theristus* sp.			Grainger et al. (1985)